Differential Transcriptomic Profiles in Canine Intestinal Organoids Following Lipopolysaccharide Stimulation

Dipak K. Sahoo
Iowa State University
Dana C. Borcherding
Iowa State University
Lawrance Chandra
Iowa State University
Albert E. Jergens
Iowa State University
Todd Atherly
Iowa State University
Agnes Bourgois-Mochel
Iowa State University
Andrew J. Severin
Iowa State University
Matthew Ellinwood
Iowa State University
Elizabeth Snella
Iowa State University
Martin Martin
Mayo Clinic
Karin Allenspach (allek@iastate.edu)
Iowa State University
Jonathan P. Mochel
Iowa State University

Research Article

Keywords: LPS, enteroids, colonoids, IBD, Mast cell tumor, Canine, Microarray

Posted Date: January 5th, 2022

DOI: https://doi.org/10.21203/rs.3.rs-967308/v1

Abstract

Lipopolysaccharide (LPS) is associated with chronic intestinal inflammation and promotes intestinal cancer progression in the gut. While the interplay between LPS and intestinal immune cells has been well characterized, little is known about LPS and intestinal epithelium interactions. In this study, we explored the differential effect of LPS on proliferation and the transcriptome in 3D enteroids/colonoids obtained from dogs with naturally occurring gastrointestinal (GI) diseases, such as Inflammatory Bowel Disease (IBD) and GI mast cell tumor. The study objective was to analyze LPS-induced modulation of signaling pathways involving the intestinal epithelia and critical to colorectal cancer development in the context of IBD or a tumor microenvironment. While LPS incubation resulted in a pro-cancer gene expression pattern and stimulated proliferation of IBD enteroids and colonoids, down-regulation of several cancer-associated genes like *CRYZL1*, *Gpatch4*, *SLC7A1*, *ATP13A2*, and *ZNF358* was also observed in tumor enteroids. Genes participating in porphyrin metabolism (*CP*), thiamine and purine metabolism (*TAP2*, *EEF1A1*), arachidonic acid, and glutathione metabolism (*GPX1*) exhibited a similar pattern of altered expression between IBD enteroids and IBD colonoids following LPS stimulation. In contrast, genes involved in anion transport, transcription and translation, apoptotic processes, and regulation of adaptive immune responses showed opposite expression patterns between IBD enteroids and colonoids following LPS treatment. In brief, the cross-talk between LPS/TLR4 signal transduction pathway and several metabolic pathways, such as fatty acid degradation and biosynthesis, and purine, thiamine, arachidonic acid, and glutathione metabolism, may be important in driving chronic intestinal inflammation and intestinal carcinogenesis.

Introduction

Lipopolysaccharide (LPS) is the most effective cell wall-derived inflammatory toxin of Gram-negative bacteria with its inner component, lipid A, accountable for most of the toxin's inflammatory effects[1]. The intestinal lumen, a habitat for many trillions of commensal bacteria, is the primary LPS reservoir in the body[2]. During normal circumstances, the intestinal epithelium retains proper barrier function by promoting the transcellular movement of nutrients, water, and ions while reducing paracellular transport of bacteria or its products/toxins (including LPS) into the systemic circulation[3]. In intestinal permeability disorders, such as infection by pathogenic bacteria, and faulty detoxification of LPS, the defective tight junctions (TJ) barrier will permit enhanced paracellular flux of LPS and other phlogistic luminal antigens[4]. Interestingly, apical but not basolateral exposure to LPS, induces epithelial apoptosis through caspase-3 activation and stimulates disruption of tight junctional ZO-1, thus increasing epithelial permeability[5]. While transported in blood, LPS binds to either LPS binding protein (LBP) or plasma lipoproteins and induces systemic inflammation[4]. Basically, LPS-induced intestinal inflammation occurs through stimulation of toll-like receptor 4 (TLR4), which subsequently leads to recruitment of intracellular nuclear transcription factor-κB (NF-κB) followed by the release of chemokines and inflammatory cytokines including necrosis factor-alpha (TNF-α)[6]. TNF-α is accountable for various signaling events within cells, leading to necrosis or apoptosis, therefore playing a pivotal role in resistance to infection and cancers. Activation of the TLR-4 dependent FAK-MyD88-IRAK4 signaling pathway controls LPS-induced intestinal inflammation and tight junction permeability[7,8].

The removal of circulating LPS (via amelioration of dysbiosis) facilitates the clinical recovery of inflammatory bowel disease (IBD), demonstrating its significant role in mediating chronic intestinal inflammation in IBD[2]. The role of LPS throughout the body has been well studied in the context of activation of immune cells (macrophages, dendritic cells, and T cells), where it causes pleiotropic inflammatory cytokine and chemokine secretion[9]. While LPS

interactions with intestinal macrophages, dendritic cells, and T cells are well characterized[10,11], few studies have investigated the direct interactions between LPS and the intestinal epithelium. Regardless of the significance of an impaired intestinal barrier in the development of intestinal inflammation in IBD, the effect of increased circulating levels of LPS on the intestinal epithelial barrier integrity remain mostly unknown. Concurrence of IBD among monozygotic vs. dizygotic twin pairs has validated the possible role of genetics in IBD development, with a frequency of 50–55% being detected[12]. Since the circulating LPS level is significantly elevated in IBD patients, a greater understanding of the role of LPS on intestinal gene expression modulating intestinal barrier function has important clinical implications.

As a trigger of inflammatory responses, LPS has been associated with cancer pathogenesis, including the development of gastrointestinal (GI) mast cell tumors and colorectal cancer (CRC)[13–15]. Different microbial products and TLR4 agonists have demonstrated the crucial role of TLR4 signaling in regulating tumor growth, survival, and progression in colonic, pancreatic, liver, and breast cancers[16]. The TLR4 signaling pathway has been shown to drive tumorigenesis and exhibit some antitumor effect on TLR4 activation[17,18]. Gene expression profiling using microarray technology has been applied to identify physiologically and clinically significant subgroups of TNF-responsive tumors, elucidate the combinatorial and complex nature of cancers,[19,20] and advance our mechanistic understanding of oncogenesis.

The dog genome and its organization have been studied extensively in the last ten years. For understanding the biology and human diseases, dogs have emerged as a primary large animal model[21–25]. Of the large animal models used in translational GI research, the dog is particularly relevant since it presents similar gut physiology, dietary habits, and intestinal microbiota to humans[23,26]. Moreover, dogs spontaneously acquire severe chronic intestinal diseases such as IBD and CRC, which make them ideal animal models for translational GI research[25]. Our laboratory has successfully developed and characterized a canine 3D enteroids/colonoids model system to study intestinal biology during health and disease, and bridge the translational knowledge gap between mice and human[24,27]. Adult stem cell-derived intestinal organoids have previously been shown to retain their genetic and epigenetic phenotype *in vitro* after numerous passages[28]. We, therefore, hypothesized that a stromal mast cell tumor in the small intestine of a dog could influence the phenotypic expression of the overlying epithelium, which would be retained in organoid culture. Mast cell tumors are known to secret histamine, proteases, prostaglandin D2, leukotrienes, heparin, as well as a variety of pro-inflammatory cytokines[29], which could change the expression profile of the epithelium overlying the tumor and priming it to be sensitized to LPS. This study aimed to broaden our understanding of LPS-induced regulation of signaling pathways in the intestinal epithelium and identify novel genes involved in inflammatory disease and colorectal cancer development.

Materials And Methods

Ethical animal use

The collection and analysis of intestinal biopsy samples from dogs with IBD and mast cell tumors were previously approved by the Iowa State University (ISU) Institutional Animal Care and Use Committee (IACUC-19-102; PI: Albert E. Jergens). All methods were performed in accordance with the relevant guidelines, and regulations of IACUC as required by U.S. federal regulations[30]. The study is reported in accordance with ARRIVE guidelines (https://arriveguidelines.org).

Crypt cell isolation and enrichment for enteroid and colonoid culture

Ten to fifteen endoscopic mucosal biopsies (using 2.8/3.2 mm forceps cup) of the ileum and colon were obtained from two dogs, one diagnosed with IBD (to derive colonoids) and another one with a mast cell tumor (to derive enteroids/colonoids). Epithelial crypts were isolated and enriched from intestinal biopsy samples, as reported previously[31]. Briefly, ileal and colonic biopsies were cut into small pieces (1-2 mm thickness) with a scalpel and were washed six times using the complete chelating solution (1X CCS). Pre-wetted pipette and conical tubes with 1% Bovine Serum Albumin (BSA) were used throughout the procedure to prevent the adherence of the crypt epithelia in the tubes and pipette, thereby minimizing loss of cryptal units[31]. Then, tissues were incubated with 1X CCS containing EDTA (20mM- 30mM) for 45 minutes for colonic biopsies and 75 minutes for ileal biopsies at 4°C on a 20-degree, 24 rpm mixer/rocker (Fisher). After EDTA chelation, the cryptal epithelia release was augmented by trituration and/or mild shaking with a vortex. Additional trituration and/or mild shaking was performed after adding 2 mL of fetal bovine serum (FBS, Atlanta Biologicals) to maximize the number of isolated crypts. After tissue fragments settled to the bottom of the tube, the crypt suspension containing supernatant was transferred to a new conical tube then centrifuged at 150g, 4°C for 10 minutes. After centrifugation, the supernatant was removed, and the cell pellet was washed with 10 mL complete medium without an ISC growth factor (CMGF-) medium by repeating the centrifugation and decantation of the supernatant. Following crypt pellet washing, the cell pellet was re-suspended in 2 mL CMGF- medium, and the approximate number of crypt units isolated was enumerated using a hemocytometer[24].

An estimated 50-100 crypts were seeded per well in 30 µL of Matrigel (Corning® Matrigel® Growth Factor Reduced [GFR] Basement Membrane Matrix) into a 24 well plate format and incubated at 37°C for 10 minutes[31]. 0.5 mL of complete medium with ISC growth factor (CMGF+) medium with the rho-associated kinase ROCK-I inhibitor Y-27632 (StemGent) and glycogen synthase kinase 3β inhibitor CHIR99021 (StemGent) was added to each well and placed in tissue culture incubator. The CMGF + medium with ROCK-I inhibitor and glycogen synthase kinase 3β inhibitor was used for the first two days of ISC culture to enhance ISC survival and prevent apoptosis. After two days, the enteroid and colonoid cultures were replenished with CMGF + medium every two days for 6-7 days. These freshly isolated 3D enteroid and colonoid cultures were termed Passage-0 (P0).

For subsequent passaging, enteroids and colonoids in Matrigel media were mechanically disrupted using a 1 mL syringe with a 23g ¾” needle (trituration), collected into a 15 mL conical tube and washed with CMGF- medium, then pelleted by centrifugation at 4°C x 100 g for 10 minutes. The pelleted enteroids and colonoids were cultured as previously described and designated as P1. This process was repeated for additional cell culture passages.

LPS stimulation of canine enteroids and colonoids

After four passages, colonoids from a dog with IBD and enteroids and colonoids from a dog diagnosed with an intestinal mast cell tumor were grown on 18 wells of a 24 well culture plate. Among the 18 wells, 9 wells served as control cultures while 9 wells served as LPS treated cultures for these experiments. To investigate the influence of a tumor microenvironment on the intestinal epithelium, we utilized enteroids from a canine intestinal mast cell tumor. In control enteroid/colonoid cultures, the culture wells were treated with only CMGF+ medium, whereas the LPS treatment group received CMGF+ medium added with LPS at a concentration of 5 µg/ml. A high dose of LPS (5 µg/ml) was used to mimic the high concentration of bacterial-derived luminal LPS[32]. After 48 hours[33], photographs of culture wells containing the organoids were obtained using a phase-contrast microscope, and the culture media was collected and stored. All enteroids and colonoids from the separate 9 well groups were pooled and washed

with PBS and then homogenized in TRIzol (Invitrogen™:TRIzol™ Reagent # 15596026) for microarray and quantitative real-time PCR (qPCR) analyses.

These samples were labeled separately (1-6) to avoid bias in interpretation and described below:

Description of the Sample	Sample Designation
Control enteroids from MC tumor environment (9 biological replicates (wells) pooled together)	Sample-1
LPS treated enteroids from the MC tumor environment (9 biological replicates (wells) pooled together)	Sample-2
Control enteroids from IBD dogs (9 biological replicates (wells) pooled together)	Sample-3
LPS treated enteroids from IBD dogs (9 biological replicates (wells) pooled together)	Sample-4
Control colonoids from IBD dogs (9 biological replicates (wells) pooled together)	Sample-5
LPS treated colonoids from IBD dogs (9 biological replicates (wells) pooled together)	Sample-6

MC = mast cell

RNA extraction and Affymetrix Canine Genome 2.0 Array microarray processing

Total RNA, including microRNA, was isolated from these six samples using the miRNeasy Mini Kit (QIAGEN # 217004) following manufacturers' instructions. Extracted RNA was quantitated, and the purity was evaluated using Synergy H1 Hybrid Multi-Mode Reader (BioTek). The high-quality RNA samples were then analyzed by the Gene Expression and Genotyping Facility of the Case Comprehensive Cancer Center in Cleveland, OH. The samples were further purified using Qiagen miniprep RNA clean up (Qiagen) as per Affymetrix protocols for array preparation. Purified RNA samples were quantified and assessed for quality using a Bioanalyzer 2100 instrument (Agilent Technologies, Palo Alto, CA). 0.1 µg of purified RNA was reverse transcribed and used to make cRNA. According to the manufacturer's instructions, samples were hybridized to Canine Genome Version 2.0 Affymetrix oligonucleotide arrays (Affymetrix, Santa Clara, CA).

Assessment of cell proliferation by qPCR

As per the manufacturer's instructions, samples containing 0.5 µg of total RNA were used to synthesize cDNA by iScript™ Advanced cDNA Synthesis Kit (Bio-Rad, Life Science, Hercules, California). Real-time PCR for Ki-67 expression was carried out using the synthesized cDNA using PowerUp SYBR Green Master Mix following the manufacturer's protocol. Thermocycling conditions were as follows: 50°C for 2 minutes and then 95°C for 2 minutes, followed by 35 cycles of 95°C for 15 seconds and 60°C for 1 minute. The expression of *Ki-67* in cell cultures was normalized using *GAPDH* and quantified using the delta-delta Ct method[34]. Details of the primers and primer optimization are provided in the supplementary material.

Analysis of microarray data

Microarray CEL files were processed using the R library affylmGUI. Contrasts were computed as given below;

1. Sample 2 vs. Sample 1

2. Sample 4 vs. Sample 3
3. Sample 6 vs. Sample 5
4. Sample 5 vs. Sample 3
5. Sample 3 vs. Sample 1
6. Sample 6 vs. Sample 4
7. Sample 4 vs. Sample 2

AffylmGUI[35] was used to analyze the microarray data. The quality of the microarray chips was determined by NUSE and RNA degradation plots. Probe level data was converted into probe set expression data and normalized using GCRMA. Contrasts between treatment and control were made using the built-in linear model of affylmGUI. Since pooled data was used without replication, there were no replicates, and Empirical Bayes statistics could not be computed. MA plots were generated in R, where M is the $\log_2$ ratio of probe intensity, and A is the average probe intensity in the contrast (Table-S10; Probe IDs and their associated gene information are available: https://www.ebi.ac.uk/arrayexpress/files/A-AFFY-149/A-AFFY-149.adf.txt). The MA plot shows a cone shape where $\log_2$ fold change M decreases with average probe intensity A. Probes that were on the edge of this cone shape are of potential interest as they fall outside the bulk of the probes for a given intensity. Therefore, to identify probes of interest, the hexbin library in R was used to identify probes that fall in low-density regions of the MA plot, which corresponds to the edges of the MA plot[36]. This method was chosen to select probes without bias and for reproducibility. One advantage of this approach is that the probes that are most different in a comparison of samples will be identified. However, one point of caution is that regardless of the M value magnitude for all sample comparisons, there will still be a relatively small number of probes identified (~500). KEGG ids from these probes were explored using GenomeNet Kegg pathway search.

BLAST search and KEGG pathway analyses

Blast2GO was used to determine the function and localization of differentially expressed genes (DEGs)[37]. It is a widely used annotation platform that uses homology searches to associate sequence with Gene Ontology (GO) terms and other functional annotations. Blast2GO generated gene ontology annotations were determined for the three sub-trees of GO, (a) biological process, (b) molecular function (c) cellular component. The KEGG (Kyoto Encyclopedia of Genes and Genomes)[38,39] pathway analyses were performed by Blast2GO.

Results

LPS stimulates higher intestinal epithelial cell proliferation

LPS at a concentration of 5 µg/ml caused an increase in the size and numbers of canine enteroids and colonoids, which were apparent under phase-contrast microscopy (**Fig. 1a**). Although all enteroids and colonoids showed increased proliferation following LPS stimulation, the magnitude of proliferation was higher in tumor enteroids, followed by IBD enteroids and IBD colonoids. To confirm the magnitude of increased proliferation of enteroids and colonoids after LPS stimulation, qPCR was used to evaluate mRNA expression of Ki-67, a nuclear proliferation marker[40]. LPS stimulation caused a 4-fold increase in Ki-67 mRNA expression in tumor enteroids and a 3.4-fold increase in IBD enteroids, whereas LPS caused a 1.7-fold increase in IBD colonoids (**Fig. 1b**).

Microarray analysis reveals differential expression of genes stimulated by LPS in IBD intestinal organoids and tumor enteroids

In this study, we used GeneChip® Canine Genome 2.0 Array that contains more than 42,800 *Canis familiaris* probe sets to evaluate gene expression[41]. These probe sets targeted more than 18,000 *C. familiaris* mRNA/EST-based transcripts and more than 20,000 non-redundant predicted genes for more comprehensive coverage[41]. We performed multiple comparisons between samples to determine the effect of LPS treatment, anatomical location, and the *in vivo* microenvironment (tumor/IBD) on mRNA expression profiles of organoids following LPS stimulation. The highest number of highly differentially expressed mRNAs (684) was found in LPS-treated IBD colonoids vs. Control IBD colonoids (**Table 1**). Among this total number of highly differentially expressed mRNAs, 48% were upregulated, and 52% were down-regulated (**Table 1**). Although similar numbers of differentially expressed mRNAs (677) were found between LPS-treated tumor enteroids vs. control tumor enteroids, 56% were upregulated, and 44% were downregulated.

The next highest number of differentially expressed mRNAs (639) was found between LPS treated IBD enteroids vs. control untreated IBD enteroids (**Table 1**). Of the differentially expressed mRNAs, 49% were upregulated, and 51% were down-regulated (**Table 1**). Interestingly, between LPS treated IBD colonoids and enteroids, only 421 differentially expressed mRNAs were identified, of which 39% were upregulated, and 61% were downregulated. LPS stimulation caused 314 differentially expressed mRNAs in IBD enteroids vs. LPS treated tumor enteroids. Among these differentially expressed mRNAs, 51% were upregulated, and 49% were downregulated. Furthermore, LPS stimulation resulted in a unique transcriptomic heat map for tumor enteroids, IBD enteroids, and colonoids (**Supplemental Fig. S1**).

Comparison of gene expression profiles in tumor enteroids with and without LPS stimulation

Genes that demonstrated high levels of activity in tumor enteroids following LPS stimulation included Src-associated-substrate-during-mitosis-of-68kDa/KH domain-containing RNA binding, signal transduction associated 1 (*Sam68/KHDRBS1*), Flap endonuclease GEN homolog 1 (*GEN1*), krev interaction trapped-1 (*KRIT1*), Centromere protein F (*CENPF*) and tyrosine-protein kinase (*STYK1*). However, expressions of quinone oxidoreductase-like protein 2/Crystallin Zeta Like 1 (*CRYZL1*), G patch domain-containing protein 4 (*Gpatch4*), Solute Carrier Family 7 Member 1/high-affinity cationic amino acid transporter 1 (*SLC7A1*), cation-transporting ATPase 13A2 (*ATP13A2*), and zinc finger protein 358 (*ZNF358*) genes were significantly repressed in LPS-treated tumor-adjacent enteroids (**Fig. 2**).

Blast2GO functional group analysis

Using the Blast2GO functional group analysis[37,39] (**Fig. 3; Table S1**), the highly differentially expressed genes (DEGs) stimulated by LPS treatment on tumor enteroids were predominantly overrepresented in the cellular component category for intracellular organelle (12%), intracellular non-membrane-bounded organelle (7%), membrane-bounded organelle (7%), an integral component of membrane (7%), non-membrane-bounded organelle (7%), plasma membrane (5%) and centromere (5%) (**Fig. 3**). In comparison, the categories corresponding to identical protein binding (10%) and nucleic acid binding (10%) were significantly overrepresented in molecular function. Nitrogen compound metabolic process (7%), cell cycle process (3%), regulation of molecular function (3%), and cellular homeostasis (3%) were overrepresented for biological process (**Fig. 3**; **Table S1**).

Notably, the Blast2GO analysis revealed numerous genes involved in various biological processes, and these genes were significantly affected by LPS-induced inflammation, inflammatory bowel disease, and carcinogenesis (**Fig. 3-5**, **Fig. S2-9**, **Table S1-S10**). Changes in genes associated with cellular metabolic processes, stress response, cell death, and immune response were primarily overrepresented in the biological process category; intracellular organelle, extracellular region, and plasma membrane were overrepresented in the cellular component category; and transferase activity, one-carbon group transfer, and metal ion binding were overrepresented in the molecular function category (**Fig. S1-S10**).

Genes showing similar expression patterns between IBD enteroids and colonoids following LPS stimulation

The pattern of gene expression was compared between LPS-stimulated IBD enteroids and colonoids. We identified 34 genes across these two groups with similar expression patterns (**Fig. 6** & **Table 2-3**). Following LPS stimulation, 13 of these 34 genes were elevated in both IBD enteroids and colonoids, whereas 21 were downregulated. These 34 genes may represent the intestinal epithelium signature LPS responsive gene network, regardless of the intestinal regions.

Following LPS stimulation of IBD enteroids and colonoids, significant up-regulation of genes involved in stress response (*OAS1*, *OASL*, *IFIT1*, *GPX1*, and *ISG15*) was observed, despite the fact that several of these genes (*OAS1*, *OASL*, and *ISG15*) and *EEF1A1* were previously implicated in primary metabolic processes and their regulation. Additional upregulated genes include those involved in the cellular response to stimulus (*TFF1*, *IFIT1*, *ISG15*, *GPX1*, *IGFBP1*), signal transduction (*TFF1*, *IGFBP1*, *ISG15*), response to biotic stimulus, immune effector process, immune system regulation, immune system development/cytokine production (*OAS1*, *OASL*, *IFIT1*, *ISG15*), antigen processing and presentation (*TAP2*, *DLA class I*), and oxidation-reduction process and cellular detoxification (*CP*, *GPX1*), regulation of molecular function (*OASL*, *IFIT1*, *NOXO1*), transmembrane transport (*TAP2*), cell motility (*S100A2*) and positive regulation of viral process (*IFIT1*) (**Fig. 4**, **Fig. 6** and **Table-S8**). On the other hand, considerable down-regulation of the *RPS24* and *ATP1A1* genes, involved in primary metabolic processes and transmembrane transport, respectively, was observed (**Fig. 4** & **Fig. 6**).

Genes upregulated in IBD enteroids and down-regulated in IBD colonoids (and vice versa) following LPS stimulation

Interestingly, 18 genes were found to be altered in the opposite direction (**Fig. 5** & **7**, & **Table-2-3** & **S9**). These 18 genes were elevated in LPS-treated IBD enteroids; however, these same 18 genes were down-regulated in LPS-treated colonoids. These findings imply that a distinct gene signature might be utilized to differentiate the intestinal region in response to LPS stimulation.

The LPS-stimulated genes that exhibit opposite expression trends between IBD enteroids and colonoids are involved in anion transport (*TOMM20*, *ANXA1*, *KPNA2*), translation (*RPS20*, *EIF3F*, *MRPS21*), protein import (*TOMM20*, *KPNA2*), protein-containing complex assembly (*TOMM20*, *SF3A1*), regulation of proteolysis (*LOC111092171*, *HSPD1*), RNA metabolic process (*GTF2A2*, *SF3A1*), positive regulation of leukocyte cell-cell adhesion, T cell activation, apoptotic process and regulation of adaptive immune response (*ANXA1*, *HSPD1*) as shown by Blast2GO analyses[37,39] (**Fig. 5** & **7**, **Table-S9**). In IBD colonoids, LPS treatment increased the expression of *EIF3F*, *ANXA1*, *SF3A1*, and *LOC111092171* genes, whereas it decreased their expression in IBD enteroids (**Fig. 7**). In contrast, the expression of *RPS20*, *MRPS21*, *TOMM20*, *KPNA2*, *HSPD1*, and *GTF2A2* genes was elevated and reduced in LPS treated IBD enteroids and colonoids, respectively (**Fig. 7**). These unique gene expression signatures

in IBD enteroids and colonoids treated with LPS may provide critical insights into intestinal physiology and novel inflammatory pathways that may serve as future drug discovery targets.

KEGG pathway analyses

KEGG pathway analysis revealed that LPS-induced DEGs were linked with thiamine and purine metabolism (*ATP13A2*), arginine biosynthesis (*OTC*), porphyrin metabolism (*CP*), and glycerophospholipid metabolism (*ENPP6*) in tumor enteroids and IBD intestinal organoids (**Table-4**).

While genes involved in nitrogen metabolism, drug metabolism, bisphenol degradation (*CA1*), arginine and proline metabolism (*ANPEP*), primary bile acid biosynthesis, taurine and hypotaurine metabolism (*BAAT*) responded in IBD intestinal organoids and tumor enteroids, LPS treatment modulated expression of *ACSL5*. *ACSL5* is involved in the degradation and biosynthesis of fatty acids, as well as the purine and thiamine metabolism pathways (**Fig. S10** & **Table-4**). *FAR1* was strongly expressed in untreated tumor enteroids and was found to be involved in wax production, as demonstrated by KEGG pathway studies (**Table-4**). Following LPS stimulation, genes involved in porphyrin metabolism (*CP*), thiamine and purine metabolism (*TAP2*, *EEF1A1*), arachidonic acid, and glutathione metabolism (*GPX1*) expressed similarly in IBD enteroids and colonoids (**Table-4**).

EggNOG Annotation

Functional gene annotation was carried out against the eggNOG (evolutionary genealogy of genes: Non-supervised Orthologous Groups) database[39,42]. In order to focus on potentially functional activities of the genes in response to LPS stimulation in IBD enteroids and colonoids, and characterize their evolutionary significance, we extracted and grouped genes in four general categories: (A) information storage and processing genes (representing 37.93% of all functional genes identified), including Transcription, translation, ribosomal structure and biogenesis and RNA processing and modification, (B) cellular processes and signaling (representing 34.48% of all functional genes identified) including intracellular trafficking, secretion, and vesicular transport, Signal transduction mechanisms, posttranslational modification, protein turnover, chaperones and extracellular structures (C) metabolism (representing 10.34%) including secondary metabolites biosynthesis, transport and catabolism, Inorganic ion transport and metabolism, and energy production and conversion and (D) genes poorly characterized or with unknown functions (representing 10.34% of all functional genes identified in both IBD enteroids and colonoids) (**Supplemental Information-1**). Out of 29 identified genes stimulated in both IBD enteroids and colonoids, 29 genes were 10.74% orthologous in Vertebrata/ Chordata/ Mammalia/ Bilateria/ Metazoa/ Opisthokonta. In comparison, 22 genes were 8.15% orthologous in Carnivora, 6 genes were 2.22% orthologous among Euarchontoglires, and 5 genes were 1.85% orthologous among Rodentia as well identified (**Supplemental Information-1**)[39,42].

Discussion

In this study, we generated enteroids and colonoids from dogs diagnosed with IBD or intestinal mast cell tumor. The goal of these experiments was to better understand how intestinal epithelial cells respond to LPS stimulation under different pathological conditions. We further investigated differences between organoids derived from various intestinal compartments (small intestine vs. colon) in IBD dogs following LPS stimulation. Transcriptomic analyses using microarray[43] were used to identify differentially expressed genes in enteroids and colonoids derived from diseased dogs. These data are the first to characterize regional specific transcriptomic changes in intestinal epithelial cells of dogs with IBD and intestinal cancer in response to *ex vivo* LPS stimulation.

In the present study, tumor enteroids had the highest proliferation indices (based on Ki-67 estimates), followed by IBD enteroids and IBD colonoids, while all enteroids and colonoids showed an increase in proliferation following LPS stimulation. Additionally, we observed that organoid proliferation varied between enteroids and colonoids from the IBD dog, with enteroids exhibiting greater proliferation than colonoids. It is possible that LPS-induced enhanced proliferation in tumor enteroids was caused by increased expression of genes involved in cell cycle process like centromere protein F (*CENPF*) and flap endonuclease GEN homolog 1 (*GEN1*) as well as a receptor protein tyrosine kinase (*STYK1*). *CENP-F* is a centromere-kinetochore complex-associated protein, and its expression is increased in tumors[44] and it serves as a marker for cell proliferation in human malignancies[45]. CRISPR-Cas9 silencing of *CENPF* in human prostate cancer cells resulted in decreased cell proliferation[46,47]. *CENPF* regulates cancer metabolism by modulating the phosphorylation signaling of pyruvate kinase M2[47].

Similarly, *GEN1* expression was induced in tumor enteroids. GEN1, like other members of the Rad2/XPG family as *FEN1*, is a monomeric 59-flap endonuclease, but it can dimerize on Holliday junctions (HJs), providing the two symmetrically aligned active sites required for HJ resolution[48]. Members of the Rad2/XPG family, such as *FEN1*, are significantly expressed in proliferating cell populations, consistent with their role in DNA replication[49]. For instance, its expression is associated with proliferation of mammary epithelial cells[49]. *FEN1* expression is increased in metastatic prostate cancer cells, gastric cancer cells, pancreatic cancer cells, and lung cancer cell lines, and with tumor progression[50]. Additionally, the receptor STYK1 is required for cell proliferation[51]. STYK1's oncogenic potential has been studied widely in gallbladder cancer (GBC) and was reported to be largely dependent on the PI3K/AKT pathway. STYK1's tumor-stimulating activity was abolished by the AKT-specific inhibitor MK2206, as well as by STYK1 gene silencing[51]. A crucial NF-κB regulator, Sam68 (KHDRBS1), was also observed to be elevated in LPS-treated tumor enteroids, along with the genes *GEN1*, *KRIT1*, *CENPF*, and *STYK1*. Sam68 (KHDRBS1) exhibited prognostic significance in various malignancies and was elevated in cancer cell lines[52,53]. Additionally, the genome-wide study identified Sam68 (KHDRBS1) co-expression with cancer-related genes[52,53]. Our results suggest the possible roles of *GEN1*, *KRIT1*, *CENPF*, *STYK1*, and *Sam68/KHDRBS1* in promoting cancer cell proliferation, and these findings may provide a potential therapeutic target to control mast cell malignancy.

While LPS treatment did not affect the expression of genes involved in proliferation and malignancy, such as *GEN1*, *KRIT1*, *CENPF*, *STYK1*, and *Sam68/KHDRBS1*, it did inhibit numerous genes implicated in tumor growth. LPS treatment, for example, reduced the expression of the *CRYZL1*, *Gpatch4*, *SLC7A1*, *ATP13A2*, and *ZNF358* genes. While *CRYZL1* was previously detected in circulating tumor cells in the blood of female cancer patients[54], *GPATCH4* was identified in melanoma patient sera and was revealed to be increased in hepatocellular carcinoma[55]. Similarly, the SLC7A1/CAT1 arginine transporter plays a critical function in colorectal cancer by increasing arginine metabolism[56]. After LPS treatment, another important gene, *ATP13A2*, was downregulated in tumor enteroids. ATP13A2 regulates autophagy, as demonstrated by ATP13A2 knockdown decreasing cellular autophagy levels, reversing ATP13A2-induced stemness in colon cancer cells with the autophagy inhibitor bafilomycin A1[57], and reduction of the volume of colon cancer xenografts in mice treated with ATP13A2 siRNA[57]. While all of these pieces of evidence point to ATP13A2 and autophagy, studies also reveal a link between the level of ATP13A2 expression and the survival rate of colon cancer patients. Colon cancer patients with elevated ATP13A2 expression display shorter overall survival than those with low ATP13A2[57]. While proliferation-promoting genes such as *GEN1*, *KRIT1*, *CENPF*, *STYK1*, and *Sam68/KHDRBS1* were elevated in LPS-treated tumor enteroids, ZNF139 expression was decreased. ZNF139 increases proliferation and prevents apoptosis by increasing Survivin, x-IAP, and Bcl-2

expression and decreasing Caspase-3 and Bax expression[58]. ZNF139 is substantially expressed in gastric cancer and is used as a prognostic marker in this disease[59].

Interestingly, while LPS treatment increased proliferation and expression of the *GEN1*, *KRIT1*, *CENPF*, *STYK1*, and *Sam68/KHDRBS1* genes, it decreased the expression of cancer-associated *CRYZL1*, *Gpatch4*, *SLC7A1*, *ATP13A2*, and *ZNF358* genes[47,51,57,59,60] in tumor enteroids. This could imply that LPS has some anticancer activity. LPS treatment has been shown to have potent anticancer effects[61,62] against adoptively transferred tumors (TA3/Ha murine mammary carcinoma) in mice[63,64]. LPS and the other two potent TLR4 agonists have been proven effective in treating a variety of carcinomas[62,65]. In addition, research on mice with lung tumors has demonstrated that a modest dose of LPS promotes tumor development, whereas a large amount induces tumor regression[63]. Plasmacytoid dendritic cells are required for LPS to exert its dose-dependent effects[63].

The addition of LPS increased the production of proteins involved in cytokine signaling, most notably interferon and interleukin signaling[66]. After LPS treatment, we observed the upregulation of genes involved in biotic stimuli and immune effector processes (*OAS1*, *OASL*, *IFIT1*, *ISG15*), as well as antigen processing and presentation (TAP2, DLA class I) and signal transduction (*TFF1*, *IGFBP1*, *ISG15*). Emerging evidence suggests that these genes increased activity contributes to the inflammatory response induced by LPS. For example, LPS and interferons highly activate the ubiquitin-like protein ISG15 and 2'-5'-oligoadenylate synthetase-like (OASL)[67,68] OASL is necessary for the antiviral signaling pathway mediated by IFNs[68], as it regulates pro-inflammatory mediators such as cytokines and chemokines[68]. Likewise, OAS1 has a strong antiviral impact both *in vivo* and *in vitro*[69] and protects cells from viral infection[70]. When exogenous recombinant OAS1 was added to cultured cells, it was internalized and exerted a potent antiviral effect[69]. LPS has also been shown to induce OAS in marine sponges[71]. Notably, we found that most of these DEGs are 10.74% orthologous in Metazoa.

TAP2 and trefoil factor 1 (TFF1) upregulation in IBD enteroids and colonoids following LPS treatment could result from their ability to modulate TLR4 signaling or their anti-inflammatory properties[72–74]. TAP2 has been shown to inhibit TLR4 signaling and diminish the systemic cytokine response induced by LPS[72]. TFF1 exhibits anti-inflammatory properties, and its involvement as a tumor suppressor gene has been shown through studies using the Tff1-knockout (Tff1-KO) mouse model[54,75]. While the Tff1-KO mice develops gastric malignancies via activation of NF-κB and chronic inflammatory pathways[73], treatment with exogenous TFFs alleviates gastrointestinal inflammation[54,76]. Insulin-like growth factor-binding protein 1 (IGFBP1) is a member of the GFBPs family of proteins that interact with Insulin-like growth factors (IGFs) to regulate their anabolic activity[77]. While LPS injection reduces circulating IGF-I levels, it increases IGFBP-1 levels[78,79]. LPS has also been shown to induce IGFBP-1 in the liver, muscle, and kidney tissues[80]. Similarly, NADPH oxidase 1 (NOX1) activity induced by LPS was detected in dendritic cells[81], corroborating our current findings. NOX1 requires two additional proteins, NOXO1 and NOXA1, and it interacts with p22phox in a complex[82]. NOX1 is triggered by the GTPase Rac, which binds directly to it or via the NOXA1 TPR domain[82].

Genes such as *CP* and *GPX1*, involved in the oxidation-reduction process and cellular detoxification, were expressed more abundantly in IBD intestine organoids following LPS treatment. The generation of reactive oxygen species (ROS) during the innate immune response to LPS is one of the anti-pathogen responses that can cause oxidative damage, and GPx-1, an antioxidant enzyme[83,84], can protect the intestine from such damage. Gpx-1 facilitates the generation of pro-inflammatory cytokines in response to LPS exposure[85]. GPx1 has been shown to regulate LPS-

induced adhesion molecule expression in endothelial cells through modulating CD14 expression. Suppression of GPx-1 promotes the expression of the CD14 gene in human microvascular endothelial cells[86]. GPx-1 deficiency increases LPS-induced intracellular ROS and CD14 and intercellular adhesion molecule-1 (ICAM-1) expression[86].

Studies have shown a connection between LPS stimulation and NO production and the Ceruloplasmin (CP) activity[87]. Without changing iNOS expression levels, CP enhances LPS-activated iNOS activity. An unknown Cp receptor activates this intracellular signaling that cross-talks with the response stimulated by LPS[88]. Members of the S100 family, S100A2 and S100A16, were also induced by LPS stimulation and IBD; similar induction of S100A2 expression induction and secretion has been reported in the previous studies[89]. S100A2 is believed to be a functional component in the immune response[89,90] due to its increased expression in LPS-stimulated immune cells. S100A2 has also been linked to cancer through regulating downstream of the BRCA1/ΔNp63 signaling axis[91]. Furthermore, our current research shows associations between S100 proteins and IBD, with LPS and IBD both stimulating S100A16 activity. Our present study, along with earlier reports[92] points to the potential use of S100 markers for diagnostic purposes, specifically S100A2 in cancer and S100A16 in IBD. Use of S100 A proteins in canine feces as biomarkers of inflammatory activity has been previously reported[93].

The transmembrane ion pump Na+/K+-ATPase (ATP1A1) has been linked to nuclear factor kappa B (NFκB) signaling[94], a signal associated with the LPS induced immune response. While α2Na+/K+-ATPase haploinsufficiency was reported to regulate LPS-induced immune responses negatively, we observed that *ATP1A1* was suppressed in both IBD enteroids and colonoids treated with LPS in the present study. Nonetheless, our demonstration of the inhibited expression of *ATP1A1* in IBD intestinal organoids identifies it as a promising candidate for further analysis.

The GI tract microbial ecology varies according to its microbial diversity and anatomic location. Oxygen tension is a primary determinate of microbial numbers and complexity[95]. The upper GI tract, stomach, and small intestine have a lower pH, shorter transit time, and reduced bacterial population. However, the colon harbors the greatest diversity of bacteria, as it has a low cell turnover rate, a low redox potential, and a longer transit time[96]. As a result of the LPS reaction, the gene expression profile of enteroids and colonoids from IBD dogs also alters. Eighteen genes were increased in IBD enteroids treated with LPS but were downregulated in colonoids treated with LPS. These 18 unique signature genes might be used to differentiate the intestinal regions in response to LPS stimulation.

The differential expression of *TOMM20* and *eIF3F* between IBD enteroids and colonoids may be a reason why IBD enteroids with higher TOMM20 expression and lower eIF3F expression proliferate more than colonoids. Mitochondrial protein, translocase of the outer mitochondrial membrane complex subunit 20 (TOMM20), promotes proliferation and resistance to apoptosis and serves as a marker of mitophagy activity[97]. Reduced *TOMM20* expression in response to LPS treatment implies that LPS activates mitophagy[98], resulting in decreased proliferation in IBD colonoids (as observed in the current study). In tumor cells, enhanced *eIF3F* expression inhibits translation, cell growth, cell proliferation and induces apoptosis, whereas knockdown of eIF3f inhibits apoptosis, displaying the role of eIF3f as an essential negative regulator of cell growth and proliferation[99,100]. Furthermore, the expression of *FAM168A(TCRP1)* in IBD enteroids implies that IBD enteroids are more protected than colonoids against LPS stimulation. FAM168A operates via the PI3K/AKT/NFKB signaling pathway and has previously been shown to protect cells against apoptosis [101].

Several genes that participated in RNA metabolism, protein synthesis, import, protein complex assembly and proteolysis, anion transport, adaptive immune response, and apoptosis were also differentially expressed in LPS-treated IBD colonoids and enteroids. For instance, LPS treatment enhanced the expression of SF3A1, S100P, CRIP1, ANXA1, and RGS2 in IBD colonoids. The presence of SF3A and SF3B is required for a robust innate immune response to LPS and other TLR agonists[102]. SF3A1, a member of the SF3A complex, regulates LPS-induced IL-6 by primarily inhibiting its production[102]. Similarly, S100 proteins are known to be secreted in response to TLR-4 activation. S100 proteins also influence proliferation, differentiation, and apoptosis, in addition to inflammation[90]. Earlier reports and our recent observation of enhanced cysteine-rich intestinal protein 1 (CRIP1) expression in response to LPS suggest that CRIP may play a role in immune cell activation or differentiation[103]. While CRIP1 is abundant in the intestine[104], it is abnormally expressed in certain types of tumor[103]. CRIP1 inhibits the expression of Fas and proteins involved in Fas-mediated apoptosis[103]. LPS activates the AnxA1 gene significantly, and in the absence of AnxA1, LPS induces a dysregulated cellular and cytokine response with a high degree of leukocyte adhesion. The protective role of AnxA1 was demonstrated in AnxA1-deficient mice. In AnxA1-deficient mice, LPS induced a toxic response manifested by organ injury and lethality, restored by exogenous administration of AnxA1[105,106].

In contrast, following LPS treatment, *GTF2A2* expression was increased in IBD enteroids. *GTF2A2* is required for NF-kB signaling in LPS-induced TNFα responsive module[107]. Additionally, LPS promoted *HSPD1* and *Cyr61* expression in IBD enteroids. *Cyr61* is known to be activated by LPS and may have pleiotropic responses to LPS[108]. Human hsp60 directly promotes nitrite production and cytokine synthesis in macrophages. Human hsp60 was found to synergize with IFN-γ in its proinflammatory activity[109]. The inflammatory response to LPS was evaluated in *RGS2*$^{-/-}$. It showed that it exhibited higher expression of TNF-α and phosphorylated p38 levels in cardiomyocytes. This study demonstrates that *RGS2* plays a function in cardioprotection and anti-inflammatory signaling via p38[110]. *RGS2* inhibits G protein-coupled receptor signaling by increasing the rate of G protein deactivation or by decreasing G protein-effector interactions[111].

The KEGG[38] pathway analysis displayed that LPS induction modified the expression of thiamine, purine, and porphyrin metabolic pathway genes in tumor enteroids and IBD intestinal organoids but altered the expression of glycerophospholipid metabolism and arginine biosynthesis pathway genes in tumor enteroids. Purine metabolism is implicated in a variety of inflammatory diseases, including IBD[112]. Purine metabolism regulates innate lymphoid cell function by balancing the levels of eATP and adenosine via the NTPDase enzyme and protects against intestinal injury[112]. As the co-enzyme of pyruvate dehydrogenase and α-ketoglutarate dehydrogenase, thiamine plays a key role in carbohydrate metabolism. Accumulation of LPS results in a decrease in thiamine content and transport[113]. When thiamine-degrading enzyme thiaminase was introduced to cell culture media containing thiamine, it inhibited the growth of breast cancer cells[114]. In cancer cells, thiaminase reduced ATP levels signify its vital role in cancer cell bioenergetics[114,115]. LPS-induced TNF-α production in mice was inhibited by porphyrins suggesting its inhibitory effects in TNF-α cytokine production[116,117].

LPS treatment also altered expression of arachidonic acid and glutathione metabolism pathway genes in IBD enteroids and colonoids. The arachidonic acid (AA) pathway is implicated in a variety of inflammatory diseases[118,119]. The glutathione (GSH) pathway is a critical metabolic integrator in T cell-mediated inflammatory responses[120]. Metabolism of AA results in reactive oxygen species (ROS) generation[121]. GSH and its metabolic enzymes protect tissues from oxidative damage[83,84,122–127]. By interacting in both the AA and GSH pathways,

GPX1 is a critical determinant of AA effects[121]. Fatty acyl-CoA reductase 1 (FAR1) expression was greater in IBD enteroids than tumor enteroids. In mammals, fatty alcohol synthesis is accomplished by two highly expressed FAR isozymes[128]. FAR1 is a potential tumor suppressor, and its increased expression has been associated with improved survival rates in colorectal and breast cancer patients[129]. The enzymes of wax biosynthesis and its association with cancer have been previously reported[128,130].

As inflammation is a prominent regulator of drug-metabolizing enzymes[131], DEGs involved in drug metabolism were identified in IBD intestinal organoids and tumor enteroids. Additionally, LPS treatment altered Acyl-CoA synthetase 5 (ACSL5) expression in the intestine and tumor enteroids. ACSL5 is required for the *de novo* synthesis of lipids and fatty acid degradation, and its role in inflammation and cancer development has been reported. ACSL5 interacts with proapoptotic molecules and suppresses proliferation[132]. Following LPS treatment, genes involved in glutathione metabolism and arginine biosynthesis pathways were significantly altered in serum, whereas genes involved in the bile acid biosynthesis pathway were significantly changed in numerous rat tissues[133]. We also observed alterations in the expression of genes involved in these metabolic pathways in IBD intestinal organoids stimulated with LPS. Similarly, intestinal inflammation affects multiple metabolic pathways[134], as evidenced in IBD enteroids and colonoids that express DEGs from primary metabolic process.

In conclusion, the current study provides new and comprehensive data describing how LPS induces differential gene expression in intestinal organoids derived from dogs with chronic intestinal inflammation and small intestinal cancer. The cross-talk between LPS/TLR4 signal transduction pathway and other metabolic pathways like fatty acid degradation and biosynthesis, purine, thiamine, arachidonic acid, and glutathione metabolism demonstrates an important role for LPS in chronic inflammation and carcinogenesis. Additionally, we observed contradictory effects of LPS. While it induced the proliferation and expression of several tumor-associated genes, it decreased the expression of other cancer-associated genes in tumor enteroids, including *CRYZL1*, *Gpatch4*, *SLC7A1*, *ATP13A2*, and *ZNF358*. In summary, this study may pave the way for novel approaches to developing anti-inflammatory and anticancer therapeutics.

Declarations

Acknowledgments:

We acknowledge Gene Expression and Genotyping Facility of the Case Comprehensive Cancer Center (P30 CA43703) for their support in microarray experiment. Departmental Research Start-Up Grant, ISU to KA, Miller Research Award, Office of the Vice-President for Research, ISU to JPM for funding support.

Conflict of interest disclosure: None

Author Contributions:

DKS: analysis and interpretation of data and manuscript draft. DB and LC: concept and design of the study, data acquisition, analysis and interpretation of data, and manuscript draft. DKS, TA, and ME: acquisition and analysis of data and technical support. AJS: data analysis of microarray data and data analysis support. ABM and ES: performance of clinical trials and revising manuscript. MM: inputs in study designing and revision of manuscript. KA, AJ, and JPM: concept and design of the study, interpretation of data, and critical revision of manuscript, Funding.

References

1. Heinbockel, L. *et al.* Inhibition of lipopolysaccharide- and lipoprotein-induced inflammation by antitoxin peptide Pep19-2.5. *Frontiers in Immunology* vol. 9 1704 (2018).
2. Im, E., Riegler, F. M., Pothoulakis, C. & Rhee, S. H. Elevated lipopolysaccharide in the colon evokes intestinal inflammation, aggravated in immune modulator-impaired mice. *Am. J. Physiol. Liver Physiol.***303**, G490–G497 (2012).
3. Schoultz, I. & Keita, Å. V. The Intestinal Barrier and Current Techniques for the Assessment of Gut Permeability. *Cells***9**, (2020).
4. Ghosh, S. S., Wang, J., Yannie, P. J. & Ghosh, S. Intestinal Barrier Dysfunction, LPS Translocation, and Disease Development. *J. Endocr. Soc.***4**, (2020).
5. Chin, A. C., Flynn, A. N., Fedwick, J. P. & Buret, A. G. The role of caspase-3 in lipopolysaccharide-mediated disruption of intestinal epithelial tight junctions. *Can. J. Physiol. Pharmacol.***84**, 1043–1050 (2006).
6. Liu, T., Zhang, L., Joo, D. & Sun, S.-C. NF-κB signaling in inflammation. *Signal Transduct. Target. Ther.***2**, 17023 (2017).
7. Alhmoud, P. *et al.* Activation of FAK and MyD88 TLR4 Signal Transduction Pathway Tight Junction Permeability Is Mediated by Lipopolysaccharide Regulation of Intestinal. (2021) doi:10.4049/jimmunol.1402598.
8. Guo, S. *et al.* Lipopolysaccharide regulation of intestinal tight junction permeability is mediated by TLR-4 signal transduction pathway activation of FAK and MyD88. *J. Immunol.***195**, 4999 (2015).
9. Rossol, M. *et al.* LPS-induced cytokine production in human monocytes and macrophages. *Critical Reviews in Immunology* vol. 31 379–446 (2011).
10. Ueda, Y. *et al.* Commensal microbiota induce LPS hyporesponsiveness in colonic macrophages via the production of IL-10. *Int. Immunol.***22**, 953–962 (2010).
11. Kayama, H. & Takeda, K. Functions of innate immune cells and commensal bacteria in gut homeostasis. *J. Biochem.***159**, 141–149 (2016).
12. Orholm, M., Binder, V., Sorensen, T. I. A., Rasmussen, L. P. & Kyvik, K. O. Concordance of inflammatory bowel disease among Danish twins: Results of a nationwide study. *Scand. J. Gastroenterol.***35**, 1075–1081 (2000).
13. Hand, T. W., Vujkovic-Cvijin, I., Ridaura, V. K. & Belkaid, Y. Linking the Microbiota, Chronic Disease, and the Immune System. *Trends in Endocrinology and Metabolism* vol. 27 831–843 (2016).
14. Liu, W.-T. *et al.* LPS-induced CXCR4-dependent migratory properties and a mesenchymal-like phenotype of colorectal cancer cells. *Cell Adh. Migr.***11**, 13–23 (2017).
15. Zhu, G. *et al.* Lipopolysaccharide increases the release of VEGF-C that enhances cell motility and promotes lymphangiogenesis and lymphatic metastasis through the TLR4- NF-κB/JNK pathways in colorectal cancer. *Oncotarget***7**, 73711–73724 (2016).
16. Zhao, H. *et al.* Inflammation and tumor progression: signaling pathways and targeted intervention. *Signal Transduct. Target. Ther. 2021 61***6**, 1–46 (2021).
17. Schreibelt, G. *et al.* Toll-like receptor expression and function in human dendritic cell subsets: implications for dendritic cell-based anti-cancer immunotherapy. *Cancer Immunol. Immunother. 2010 5910***59**, 1573–1582 (2010).

18. Davis, M. B. *et al.* Intratumoral Administration of TLR4 Agonist Absorbed into a Cellular Vector Improves Anti-tumor Responses. *Clin. Cancer Res.***17**, 3984 (2011).
19. Narrandes, S. & Xu, W. Gene Expression Detection Assay for Cancer Clinical Use. *J. Cancer***9**, 2249 (2018).
20. Bertucci, F. *et al.* Gene expression profiling of cancer by use of DNA arrays: How far from the clinic? *Lancet Oncology* vol. 2 674–682 (2001).
21. Gardner, H. L., Fenger, J. M. & London, C. A. Dogs as a Model for Cancer. *Annu. Rev. Anim. Biosci.***4**, 199 (2016).
22. Shearin, A. L. & Ostrander, E. A. Leading the way: canine models of genomics and disease. *Dis. Model. Mech.***3**, 27 (2010).
23. Kathrani, A., Werling, D. & Allenspach, K. Canine breeds at high risk of developing inflammatory bowel disease in the south-eastern UK. *Vet. Rec.***169**, 635–635 (2011).
24. Chandra, L. *et al.* Derivation of adult canine intestinal organoids for translational research in gastroenterology. *BMC Biol.***17**, 33 (2019).
25. Mochel, J. P. *et al.* Intestinal Stem Cells to Advance Drug Development, Precision, and Regenerative Medicine: A Paradigm Shift in Translational Research. *AAPS Journal* vol. 20 1–9 (2018).
26. Jergens, A. *et al.* Bcl-2/Caspase 3 mucosal imbalance favors T cell resistance to apoptosis in dogs with inflammatory bowel disease. *Vet. Immunol. Immunopathol.***158**, 167–174 (2014).
27. Kopper, J. *et al.* Harnessing the Biology of Canine Intestinal Organoids to Heighten Understanding of Inflammatory Bowel Disease Pathogenesis and Accelerate Drug Discovery: A One Health Approach. *Front. Toxicol.***0**, 47 (1AD).
28. Kraiczy, J. *et al.* DNA methylation defines regional identity of human intestinal epithelial organoids and undergoes dynamic changes during development. *Gut***68**, 49–61 (2019).
29. Moon, T. C., Dean Befus, A. & Kulka, M. Mast cell mediators: Their differential release and the secretory pathways involved. *Frontiers in Immunology* vol. 5 569 (2014).
30. How to Work With Your Institutional Animal Care and Use Committee (IACUC). https://ori.hhs.gov/education/products/ncstate/iacuc.htm.
31. Blutt, S. E., Crawford, S. E., Ramani, S., Zou, W. Y. & Estes, M. K. Engineered Human Gastrointestinal Cultures to Study the Microbiome and Infectious Diseases. *CMGH* vol. 5 241–251 (2018).
32. Chen, J. *et al.* Polyamines are required for expression of Toll-like receptor 2 modulating intestinal epithelial barrier integrity. *https://doi.org/10.1152/ajpgi.00201.2007***293**, 568–576 (2007).
33. Yücel, G. *et al.* Lipopolysaccharides induced inflammatory responses and electrophysiological dysfunctions in human-induced pluripotent stem cell derived cardiomyocytes. *Sci. Rep.***7**, (2017).
34. Chandra, L. C. *et al.* Chronic Administration of Δ 9 -Tetrahydrocannabinol Induces Intestinal Anti-Inflammatory MicroRNA Expression during Acute Simian Immunodeficiency Virus Infection of Rhesus Macaques . *J. Virol.***89**, 1168–1181 (2015).
35. Wettenhall, J. M., Simpson, K. M., Satterley, K. & Smyth, G. K. affylmGUI: a graphical user interface for linear modeling of single channel microarray data. *Bioinformatics***22**, 897–899 (2006).
36. Tarca, A. L., Romero, R. & Draghici, S. Analysis of microarray experiments of gene expression profiling. *Am. J. Obstet. Gynecol.***195**, 373 (2006).
37. Conesa, A. *et al.* Blast2GO: A universal tool for annotation, visualization and analysis in functional genomics research. *Bioinformatics***21**, 3674–3676 (2005).

38. Kanehisa, M., Furumichi, M., Tanabe, M., Sato, Y. & Morishima, K. KEGG: New perspectives on genomes, pathways, diseases and drugs. *Nucleic Acids Res.***45**, D353–D361 (2017).
39. BioBam Bioinformatics. OmicsBox – Bioinformatics Made Easy. March 3, 2019 (2019).
40. Scholzen, T. & Gerdes, J. The Ki-67 protein: From the known and the unknown. *Journal of Cellular Physiology* vol. 182 311–322 (2000).
41. Affymetrix GeneChip® Canine Genome Array. http://www.affymetrix.com/products_services/arrays/specific/canine.affx#1_2.
42. Huerta-Cepas, J. *et al.* EggNOG 5.0: A hierarchical, functionally and phylogenetically annotated orthology resource based on 5090 organisms and 2502 viruses. *Nucleic Acids Res.***47**, D309–D314 (2019).
43. Lowe, R., Shirley, N., Bleackley, M., Dolan, S. & Shafee, T. Transcriptomics technologies. *PLoS Comput. Biol.***13**, e1005457 (2017).
44. Ueda, S. *et al.* Expression of centromere protein F (CENP-F) associated with higher FDG uptake on PET/CT, detected by cDNA microarray, predicts high-risk patients with primary breast cancer. *BMC Cancer***8**, 384 (2008).
45. Landberg, G., Erlanson, M., Roos, G., Tan, E. M. & Casiano, C. A. *Nuclear Autoantigen p330dKENP-F: A Marker for Cell Proliferation i n Human Malignancies*. doi:10.1002/(SICI)1097-0320(19960901)25:1.
46. Oono, K. *et al.* Inhibition of PC3 human prostate cancer cell proliferation, invasion and migration by eicosapentaenoic acid and docosahexaenoic acid. *Mol. Clin. Oncol.***7**, 217 (2017).
47. Shahid, M. *et al.* Centromere protein F (CENPF), a microtubule binding protein, modulates cancer metabolism by regulating pyruvate kinase M2 phosphorylation signaling. *Cell Cycle***17**, 2802–2818 (2018).
48. Rass, U. *et al.* Mechanism of Holliday junction resolution by the human GEN1 protein. doi:10.1101/gad.585310.
49. Sun, L. *et al.* Expression and Localization of GEN1 in Mouse Mammary Epithelial Cells. *J. Biochem. Mol. Toxicol.***28**, 450–455 (2014).
50. Ge, Y., Ezzell, R. M. & Warren, H. S. Localization of Endotoxin in the Rat Intestinal Epithelium. *J. Infect. Dis.***182**, 873–881 (2000).
51. Hu, Y. ping *et al.* STYK1 promotes cancer cell proliferation and malignant transformation by activating PI3K-AKT pathway in gallbladder carcinoma. *Int. J. Biochem. Cell Biol.***97**, 16–27 (2018).
52. Song, L. *et al.* Sam68 up-regulation correlates with, and its down-regulation inhibits, proliferation and tumourigenicity of breast cancer cells. *J. Pathol.***222**, 227–237 (2010).
53. Sumithra, B., Saxena, U. & Das, A. B. A comprehensive study on genome-wide coexpression network of KHDRBS1/Sam68 reveals its cancer and patient-specific association. *Sci. Reports 2019 91***9**, 1–10 (2019).
54. Obermayr, E. *et al.* Assessment of a six gene panel for the molecular detection of circulating tumor cells in the blood of female cancer patients. *BMC Cancer***10**, 1–12 (2010).
55. Blotta, S. *et al.* Identification of novel antigens with induced immune response in monoclonal gammopathy of undetermined significance. *Blood***114**, 3276–3284 (2009).
56. Lu, Y. *et al.* Overexpression of Arginine Transporter CAT-1 Is Associated with Accumulation of L-Arginine and Cell Growth in Human Colorectal Cancer Tissue. *PLoS One***8**, e73866 (2013).
57. Chen, Q. *et al.* Knockdown of Parkinson's disease-related gene ATP13A2 reduces tumorigenesis via blocking autophagic flux in colon cancer. (2020) doi:10.1186/s13578-020-00506-z.
58. Jen, J. & Wang, Y. C. Zinc finger proteins in cancer progression. *Journal of Biomedical Science* vol. 23 (2016).

59. Li, Y. *et al.* ZNF139 promotes tumor metastasis by increasing migration and invasion in human gastric cancer cells. *Neoplasma***61**, 291–298 (2014).
60. Lu, Y. *et al.* Overexpression of Arginine Transporter CAT-1 Is Associated with Accumulation of L-Arginine and Cell Growth in Human Colorectal Cancer Tissue. *PLoS One***8**, 73866 (2013).
61. Otto, F. *et al.* Phase II trial of intravenous endotoxin in patients with colorectal and non-small cell lung cancer. *Eur. J. Cancer***32**, 1712–1718 (1996).
62. Wiemann, B. & Starnes, C. O. Coley's toxins, tumor necrosis factor and cancer research: A historical perspective. *Pharmacol. Ther.***64**, 529–564 (1994).
63. Rega, A. *et al.* Plasmacytoid Dendritic Cells Play a Key Role in Tumor Progression in Lipopolysaccharide-Stimulated Lung Tumor–Bearing Mice. *J. Immunol.***190**, 2391–2402 (2013).
64. Rakoff-Nahoum, S. & Medzhitov, R. Toll-like receptors and cancer. *Nature Reviews Cancer* vol. 9 57–63 (2009).
65. Kaczanowska, S., Joseph, A. M. & Davila, E. TLR agonists: our best frenemy in cancer immunotherapy. *J. Leukoc. Biol.***93**, 847 (2013).
66. Kawasaki, T. & Kawai, T. Toll-Like Receptor Signaling Pathways. *Front. Immunol.***0**, 461 (2014).
67. Arya, S. *et al.* Quantitative proteomic changes in LPS-activated monocyte-derived dendritic cells: A SWATH-MS study. *Sci. Rep.***9**, 1–11 (2019).
68. Yang, C. *et al.* Identification of 2'-5'-Oligoadenylate Synthetase-Like Gene in Goose: Gene Structure, Expression Patterns, and Antiviral Activity Against Newcastle Disease Virus. *J. Interf. Cytokine Res.***36**, 563–572 (2016).
69. Kristiansen, H. *et al.* Extracellular 2'-5' Oligoadenylate Synthetase Stimulates RNase L-Independent Antiviral Activity: a Novel Mechanism of Virus-Induced Innate Immunity. *J. Virol.***84**, 11898 (2010).
70. Rysiecki, G., Gewert, D. R. & Williams, B. R. g. Constitutive Expression of a 2',5'-Oligoadenylate Synthetase cDNA Results in Increased Antiviral Activity and Growth Suppression. *J. Interferon Res.***9**, 649–657 (1989).
71. Grebenjuk, V. A. *et al.* Induction of (2'-5')oligoadenylate synthetase in the marine sponges Suberites domuncula and Geodia cydonium by the bacterial endotoxin lipopolysaccharide. *Eur. J. Biochem.***269**, 1382–1392 (2002).
72. Schiffer, R., Baron, J., Dagtekin, G., Jahnen-Dechent, W. & Zwadlo-Klarwasser, G. Differential regulation of the expression of transporters associated with antigen processing, TAP1 and TAP2, by cytokines and lipopolysaccharide in primary human macrophages. *Inflamm. Res.***51**, 403–408 (2002).
73. Soutto, M. *et al.* Loss of TFF1 is associated with activation of NF-κB-mediated inflammation and gastric neoplasia in mice and humans. *J. Clin. Invest.***121**, 1753–1767 (2011).
74. Eletto, D. *et al.* TFF1 Induces Aggregation and Reduces Motility of Helicobacter pylori. *Int. J. Mol. Sci. 2021, Vol. 22, Page 1851***22**, 1851 (2021).
75. Jiang, Y. & Yu, Y. Transgenic and gene knockout mice in gastric cancer research. *Oncotarget***8**, 3696 (2017).
76. Tran, C. P., Cook, G. A., Yeomans, N. D., Thim, L. & Giraud, A. S. Trefoil peptide TFF2 (spasmolytic polypeptide) potently accelerates healing and reduces inflammation in a rat model of colitis. *Gut***44**, 636–642 (1999).
77. Lee, S. H. *et al.* Identification of diverse adenosine-to-inosine RNA editing subtypes in colorectal cancer. *Cancer Res. Treat.***49**, 1077–1087 (2017).
78. Soto, L., Martín, A. I., Millán, S., Vara, E. & López-Calderón, A. Effects of endotoxin lipopolysaccharide administration on the somatotropic axis. *J. Endocrinol.***159**, 239–246 (1998).
79. Allard, J. B. & Duan, C. IGF-Binding Proteins: Why Do They Exist and Why Are There So Many? *Front. Endocrinol. (Lausanne).***9**, 1 (2018).

80. Fan, J., Molina, P. E., Gelato, M. C. & Lang, C. H. Differential tissue regulation of insulin-like growth factor-I content and binding proteins after endotoxin. *Endocrinology***134**, 1685–1692 (1994).
81. Matsumoto, M. *et al.* NOX1/NADPH oxidase is involved in the LPS-induced exacerbation of collagen-induced arthritis. *J. Pharmacol. Sci.***146**, 88–97 (2021).
82. Lipinski, S. *et al.* Missense variants in NOX1 and p22phox in a case of very-early-onset inflammatory bowel disease are functionally linked to NOD2. *Cold Spring Harb. Mol. Case Stud.***5**, (2019).
83. Chainy, G. B. N. & Sahoo, D. K. Hormones and oxidative stress: an overview. *Free Radic. Res.***54**, (2020).
84. Sahoo, D. K. & Roy, A. Compromised rat testicular antioxidant defence system by hypothyroidism before puberty. *Int. J. Endocrinol.***2012**, (2012).
85. Bozinovski, S., Seow, H. J., Crack, P. J., Anderson, G. P. & Vlahos, R. Glutathione Peroxidase-1 Primes Pro-Inflammatory Cytokine Production after LPS Challenge In Vivo. *PLoS One***7**, 33172 (2012).
86. Lubos, E. *et al.* Glutathione peroxidase-1 modulates lipopolysaccharideinduced adhesion molecule expression in endothelial cells by altering CD14 expression. *FASEB J.***24**, 2525–2532 (2010).
87. Lazzaro, M. *et al.* Ceruloplasmin potentiates nitric oxide synthase activity and cytokine secretion in activated microglia. *J. Neuroinflammation 2014 111***11**, 1–11 (2014).
88. Lazzaro, M. *et al.* Ceruloplasmin potentiates nitric oxide synthase activity and cytokine secretion in activated microglia. *J. Neuroinflammation***11**, 1–11 (2014).
89. Heo, S.-H., Choi, Y.-J., Lee, J.-H., Lee, J.-M. & Cho, J.-Y. S100A2 Level Changes Are Related to Human Periodontitis. *Mol. Cells***32**, 445 (2011).
90. Donato, R. S100: A multigenic family of calcium-modulated proteins of the EF-hand type with intracellular and extracellular functional roles. *International Journal of Biochemistry and Cell Biology* vol. 33 637–668 (2001).
91. Buckley, N. E., D'Costa, Z., Kaminska, M. & Mullan, P. B. S100A2 is a BRCA1/p63 coregulated tumour suppressor gene with roles in the regulation of mutant p53 stability. *Cell Death Dis. 2014 52***5**, e1070–e1070 (2014).
92. Manolakis, A. C., Kapsoritakis, A. N., Tiaka, E. K. & Potamianos, S. P. Calprotectin, calgranulin C, and other members of the s100 protein family in inflammatory bowel disease. *Digestive Diseases and Sciences* vol. 56 1601–1611 (2011).
93. Hanifeh, M. *et al.* S100A12 concentrations and myeloperoxidase activities are increased in the intestinal mucosa of dogs with chronic enteropathies. *BMC Vet. Res.***14**, (2018).
94. Xie, Z. & Askari, A. Na+/K+-ATPase as a signal transducer. *European Journal of Biochemistry* vol. 269 2434–2439 (2002).
95. Messer, J. S., Liechty, E. R., Vogel, O. A. & Chang, E. B. Evolutionary and ecological forces that shape the bacterial communities of the human gut. *Mucosal Immunol. 2017 103***10**, 567–579 (2017).
96. Hillman, E. T., Lu, H., Yao, T. & Nakatsu, C. H. Microbial Ecology along the Gastrointestinal Tract. *Microbes Environ.***32**, 300 (2017).
97. Swiader, A. *et al.* Mitophagy acts as a safeguard mechanism against human vascular smooth muscle cell apoptosis induced by atherogenic lipids. *Oncotarget***7**, 28821 (2016).
98. Luo, X. *et al.* Drp-1 as Potential Therapeutic Target for Lipopolysaccharide-Induced Vascular Hyperpermeability. *Oxid. Med. Cell. Longev.***2020**, (2020).

99. Marchione, R., Leibovitch, S. A. & Lenormand, J.-L. The translational factor eIF3f: the ambivalent eIF3 subunit. *Cell. Mol. Life Sci.***70**, 3603 (2013).
100. Yin, Y. *et al.* The function and clinical significance of eIF3 in cancer. *Gene* vol. 673 130–133 (2018).
101. Peng, B., Gu, Y., Xiong, Y., Zheng, G. & He, Z. Microarray-Assisted Pathway Analysis Identifies MT1X & NFκB as Mediators of TCRP1-Associated Resistance to Cisplatin in Oral Squamous Cell Carcinoma. *PLoS One***7**, e51413 (2012).
102. De Arras, L. *et al.* An Evolutionarily Conserved Innate Immunity Protein Interaction Network * □ S. (2013) doi:10.1074/jbc.M112.407205.
103. Zhang, L. *et al.* Cysteine-rich intestinal protein 1 suppresses apoptosis and chemosensitivity to 5-fluorouracil in colorectal cancer through ubiquitin-mediated Fas degradation. *J. Exp. Clin. Cancer Res.***38**, 1–14 (2019).
104. Hallquist, N. A., Khoo, C. & Cousins, R. J. Lipopolysaccharide regulates cysteine-rich intestinal protein, a zinc-finger protein, in immune cells and plasma. *J. Leukoc. Biol.***59**, 172–177 (1996).
105. Foo, S. L., Yap, G., Cui, J. & Lim, L. H. K. Annexin-A1 – A Blessing or a Curse in Cancer? *Trends in Molecular Medicine* vol. 25 315–327 (2019).
106. Damazo, A. S. *et al.* Critical protective role for annexin 1 gene expression in the endotoxemic murine microcirculation. *Am. J. Pathol.***166**, 1607–1617 (2005).
107. Scicluna, B. P. *et al.* Role of Tumor Necrosis Factor-α in the Human Systemic Endotoxin-Induced Transcriptome. *PLoS One***8**, e79051 (2013).
108. Jin, Y., Kim, H. P., Ifedigbo, E., Lau, L. F. & Choi, A. M. K. Cyr61 Protects against Hyperoxia-Induced Cell Death via Akt Pathway in Pulmonary Epithelial Cells. doi:10.1165/rcmb.2005-0144OC.
109. Chen, W., Syldath, U., Bellmann, K., Burkart, V. & Kolb, H. Human 60-kDa heat-shock protein: a danger signal to the innate immune system. *J. Immunol.***162**, 3212–9 (1999).
110. Linder, A., Hagberg Thulin, M., Damber, J. E. & Welén, K. Analysis of regulator of G-protein signalling 2 (RGS2) expression and function during prostate cancer progression. *Sci. Rep.***8**, 1–14 (2018).
111. Panetta, R., Guo, Y., Magder, S. & Greenwood, M. T. Regulators of G-protein signaling (RGS) 1 and 16 are induced in response to bacterial lipopolysaccharide and stimulate c-fos promoter expression. *Biochem. Biophys. Res. Commun.***259**, 550–556 (1999).
112. Crittenden, S. *et al.* Purine metabolism controls innate lymphoid cell function and protects against intestinal injury. *Immunol. Cell Biol.***96**, 1049–1059 (2018).
113. Pan, X., Nan, X., Yang, L., Jiang, L. & Xiong, B. Thiamine status, metabolism and application in dairy cows: a review. *Br. J. Nutr.***120**, 491–499 (2018).
114. Liu, S. *et al.* Sensitivity of breast cancer cell lines to recombinant thiaminase I. *Cancer Chemother. Pharmacol.***66**, 171 (2010).
115. Zastre, J. A., Sweet, R. L., Hanberry, B. S. & Ye, S. Linking vitamin B1 with cancer cell metabolism. *Cancer Metab. 2013 11***1**, 1–14 (2013).
116. Jelić, D. *et al.* Porphyrins as new endogenous anti-inflammatory agents. *Eur. J. Pharmacol.***691**, 251–260 (2012).
117. Storjord, E. *et al.* Systemic inflammation in acute intermittent porphyria: a case–control study. *Clin. Exp. Immunol.***187**, 466 (2017).

118. Wang, B. *et al.* Metabolism pathways of arachidonic acids: mechanisms and potential therapeutic targets. *Signal Transduct. Target. Ther. 2021 61***6**, 1–30 (2021).

119. Hanna, V. S. & Hafez, E. A. A. Synopsis of arachidonic acid metabolism: A review. *J. Adv. Res.***11**, 23 (2018).

120. Mak, T. W. *et al.* Glutathione Primes T Cell Metabolism for Inflammation. *Immunity***46**, 675–689 (2017).

121. Modrick, M. L. *et al.* Role of Hydrogen Peroxide and the Impact of Glutathione Peroxidase-1 in Regulation of Cerebral Vascular Tone. *J. Cereb. Blood Flow Metab.***29**, 1130 (2009).

122. Sahoo, D. K., Jena, S. & Chainy, G. B. N. *Thyroid dysfunction and testicular redox status*. *Oxidants, Antioxidants, and Impact of the Oxidative Status in Male Reproduction* (2018). doi:10.1016/B978-0-12-812501-4.00015-8.

123. Sahoo, D. K., Roy, A. & Chainy, G. B. N. Protective effects of vitamin E and curcumin on l-thyroxine-induced rat testicular oxidative stress. *Chem. Biol. Interact.***176**, (2008).

124. Chattopadhyay, S., Sahoo, D. K., Roy, A., Samanta, L. & Chainy, G. B. N. Thiol redox status critically influences mitochondrial response to thyroid hormone-induced hepatic oxidative injury: A temporal analysis. *Cell Biochem. Funct.***28**, (2010).

125. Sahoo, D. K., Roy, A., Chattopadhyay, S. & Chainy, G. B. N. Effect of T<inf>3</inf> treatment on glutathione redox pool and its metabolizing enzymes in mitochondrial and post-mitochondrial fractions of adult rat testes. *Indian J. Exp. Biol.***45**, (2007).

126. Sahoo, D. K. & Chainy, G. B. N. Tissue specific response of antioxidant defence systems of rat to experimentally-induced hyperthyroidism. *Natl. Acad. Sci. Lett.***30**, (2007).

127. Chattopadhyay, S., Sahoo, D. K., Subudhi, U. & Chainy, G. B. N. Differential expression profiles of antioxidant enzymes and glutathione redox status in hyperthyroid rats: A temporal analysis. *Comp. Biochem. Physiol. - C Toxicol. Pharmacol.***146**, (2007).

128. Cheng, J. B. & Russell, D. W. Mammalian wax biosynthesis: I. Identification of two fatty acyl-coenzyme A reductases with different substrate specificities and tissue distributions. *J. Biol. Chem.***279**, 37789–37797 (2004).

129. Cui, W., Liu, • Dong, Gu, W. & Chu, B. Peroxisome-driven ether-linked phospholipids biosynthesis is essential for ferroptosis. *Cell Death Differ.* doi:10.1038/s41418-021-00769-0.

130. Wykle, R. L., Malone, B. & Snyder, F. Acyl-CoA reductase specificity and synthesis of wax esters in mouse preputial gland tumors. *J. Lipid Res.***20**, 890–896 (1979).

131. Stanke-Labesque, F., Gautier-Veyret, E., Chhun, S., Guilhaumou, R. & Therapeutics, on behalf of the F. S. of P. and. Inflammation is a major regulator of drug metabolizing enzymes and transporters: Consequences for the personalization of drug treatment. *Pharmacol. Ther.***215**, 107627 (2020).

132. Klaus, C., Jeon, M. K., Kaemmerer, E. & Gassler, N. Intestinal acyl-CoA synthetase 5: Activation of long chain fatty acids and behind. *World J. Gastroenterol.***19**, 7369 (2013).

133. Geng, C. *et al.* Comprehensive Evaluation of Lipopolysaccharide-Induced Changes in Rats Based on Metabolomics . *J. Inflamm. Res.***13**, 477–486 (2020).

134. Sugihara, K., Morhardt, T. L. & Kamada, N. The Role of Dietary Nutrients in Inflammatory Bowel Disease. *Front. Immunol.***0**, 3183 (2019).

Tables

Table-1: Total number of differentially expressed genes within enteroids and colonoids group

Serial No	Group comparison	Total number of differentially expressed genes	Total number of upregulated genes	Total number of downregulated genes
1 (2-1)	LPS treated tumor enteroids vs. Control tumor enteroids	677	379	298
2 (4-3)	LPS treated IBD enteroids vs. Control IBD enteroids	639	312	327
3 (6-5)	LPS treated IBD colonoids vs. Control IBD colonoids	684	327	357
4 (5-3)	Control IBD colonoids vs. Control IBD enteroids	411	180	231
5 (3-1)	Control IBD enteroids vs. Control tumor enteroids	376	185	191
6 (6-4)	LPS treated IBD colonoids vs. LPS treated IBD enteroids	421	166	255
7 (4-2)	LPS treated IBD enteroids vs. LPS treated tumor enteroids	314	161	153

Table-2: List of genes in opposite or same direction (upregulated in IBD enteriods/colonoids and down regulated in tumor-adjacent organoids and vice versa) between IBD enteroids/colonoids and tumor-adjacent organoids following LPS stimulation. The log-ratio *M* values represent log(R/G) (log fold change) (Tarca et al. 2006).

Probe Set ID	Gene Description	Gene Symbol	LPS treated vs control tumor-adjacent organoids (log-ratio *M*)	LPS treated vs control IBD colonoids (log-ratio *M*)	LPS treated vs control IBD enteroids (log-ratio *M*)
Cfa.6267.3.S1_s_at	Cysteine rich protein 1 (CRIP1)	CRIP1	-0.238149286	0.43971334	-0.3231234
Cfa.758.1.S1_at	Annexin A1	ANXA1	0.309584226	0.57352154	-0.2534974
Cfa.11085.1.A1_at	Regulator of G-protein signaling 2	RGS2	-0.302506821	0.40545754	-0.2130524

Table-3: List of genes in common/same direction between IBD enteroids, colonoids and tumor-adjacent organoids following LPS stimulation. The log-ratio *M* values represent log(R/G) (log fold change) (Tarca et al. 2006).

Probe Set ID	Gene Description	Gene Symbol	LPS treated vs control IBD colonoids (log-ratio *M*)	LPS treated vs control IBD enteroids (log-ratio *M*)	LPS treated vs control tumor-adjacent organoids (log-ratio *M*)
CfaAffx.14226.1.S1_s_at	DEAD (Asp-Glu-Ala-Asp) box polypeptide 60	DDX60	0.515	0.267	0.499
CfaAffx.18742.1.S1_at	protein S100-A2	S100A2	0.306	0.185	0.215
Cfa.15462.1.A1_at	Metallothionein-1 (LOC100686073)	Mt1	-0.522	-0.489	-0.556

Table-4: KEGG enrichment analysis results by Blast2GO. The details of each KEGG Pathway are available in Figure-S10.

*The top 10 upregulated and 10 downregulated genes (from 1 to 3) and top 50 upregulated and 10 downregulated genes (from 4-7) were studied by Blast2GO.

Figures

S.No*	Group comparison	Probe Set ID	Gene Symbol	Enzyme	Pathway
1 (2-1)	**LPS treated tumor enteroids versus Control tumor enteroids**	CfaAffx.24286.1.S1_at	ATP13A2	ec:3.6.1.15 - phosphatase	Thiamine metabolism, Purine metabolism
2 (4-3)	**LPS treated IBD enteroids versus Control IBD enteroids**	CfaAffx.26061.1.S1_at	OTC	ec:2.1.3.3 - carbamoyltransferase	Arginine biosynthesis
3 (6-5)	**LPS treated IBD colonoids versus Control IBD colonoids**	CfaAffx.13209.1.S1_s_at	CP	ec:1.16.3.1 - ceruloplasmin	Porphyrin metabolism
		Cfa.6996.1.A1_at	ENPP6	ec:3.1.4.46 - phosphodiesterase	Glycerophospholipid metabolism
4 (5-3)	**Control IBD colonoids versus Control IBD enteroids**	CfaAffx.13785.1.S1_at, Cfa.6413.1.A1_at	CA1	ec:4.2.1.1 - anhydrase	Nitrogen metabolism
		CfaAffx.13785.1.S1_at	CA1	ec:3.1.1.1 - ali-esterase	Drug metabolism - other enzymes
		CfaAffx.13785.1.S1_at	CA1	ec:3.1.1.2 - A-esterase (ambiguous)	Bisphenol degradation
		Cfa.20798.1.S1_at, Cfa.3774.1.A1_s_at	ANPEP	ec:3.4.11.5 - aminopeptidase	Arginine and proline metabolism
		CfaAffx.4748.1.S1_at	BAAT	ec:2.3.1.65 - acid-CoA:amino acid N-acyltransferase	Primary bile acid biosynthesis, Taurine and hypotaurine metabolism
5 (3-1)	**Control IBD enteroids versus Control tumor enteroids**	Cfa.6413.1.A1_at	CA1	ec:4.2.1.1 - anhydrase	Nitrogen metabolism
		CfaAffx.13785.1.S1_at	CA1	ec:3.1.1.1 - ali-esterase	Drug metabolism - other enzymes
		CfaAffx.13785.1.S1_at	CA1	ec:3.1.1.2 - A-esterase (ambiguous)	Bisphenol degradation
		Cfa.20798.1.S1_at, Cfa.3774.1.A1_s_at	ANPEP	ec:3.4.11.5 - aminopeptidase	Arginine and proline metabolism

		Cfa.20396.1.S1_at	FAR1	ec:1.2.1.84 - fatty acyl-CoA reductase	Wax biosynthesis
		CfaAffx.4748.1.S1_at	BAAT	ec:2.3.1.65 - acid-CoA:amino acid N-acyltransferase	Primary bile acid biosynthesis, Taurine and hypotaurine metabolism
6 (6-4)	**LPS treated IBD colonoids versus LPS treated IBD enteroids**	CfaAffx.13785.1.S1_at, Cfa.6413.1.A1_at	CA1	ec:4.2.1.1 - anhydrase	Nitrogen metabolism
		Cfa.18640.1.S1_at	ACSL5	ec:6.2.1.3 - ligase	Fatty acid degradation, Fatty acid biosynthesis
		CfaAffx.13785.1.S1_at	CA1	ec:3.1.1.1 - ali-esterase	Drug metabolism - other enzymes
		Cfa.18640.1.S1_at	ACSL5	ec:3.6.1.15 - phosphatase	Purine metabolism, Thiamine metabolism
		CfaAffx.13785.1.S1_at	CA1	ec:3.1.1.2 - A-esterase (ambiguous)	Bisphenol degradation
		Cfa.6996.1.A1_at	ENPP6	ec:3.1.4.46 - phosphodiesterase	Glycerophospholipid metabolism
		CfaAffx.4748.1.S1_at	BAAT	ec:2.3.1.65 - acid-CoA:amino acid N-acyltransferase	Taurine and hypotaurine metabolism, Primary bile acid biosynthesis
7 (4-2)	**LPS treated IBD enteroids versus LPS treated tumor enteroids**	CfaAffx.13785.1.S1_at, Cfa.6413.1.A1_at	CA1	ec:4.2.1.1 - anhydrase	Nitrogen metabolism
		Cfa.18640.1.S1_at	ACSL5	ec:6.2.1.3 - ligase	Fatty acid degradation, Fatty acid biosynthesis
		CfaAffx.13785.1.S1_at	CA1	ec:3.1.1.1 - ali-esterase	Drug metabolism - other enzymes
		Cfa.18640.1.S1_at	ACSL5	ec:3.6.1.15 - phosphatase	Purine metabolism, Thiamine metabolism
		CfaAffx.13785.1.S1_at	CA1	ec:3.1.1.2 - A-esterase (ambiguous)	Bisphenol degradation
		Cfa.6996.1.A1_at	ENPP6	ec:3.1.4.46 - phosphodiesterase	Glycerophospholipid metabolism
		CfaAffx.4748.1.S1_at	BAAT	ec:2.3.1.65 - acid-	Primary bile acid

			CoA:amino acid N-acyltransferase	biosynthesis, Taurine and hypotaurine metabolism
Common genes between IBD enteroids and colonoids following LPS stimulation	Cfa.2878.1.A1_s_at	CP	ec:1.16.3.1 - ceruloplasmin	Porphyrin metabolism
	CfaAffx.2163.1.S1_at, CfaAffx.21951.1.S1_s_at	TAP2, EEF1A1	ec:3.6.1.15 - phosphatase	Thiamine metabolism, Purine metabolism
	CfaAffx.17868.1.S1_at	GPX1	ec:1.11.1.9 - peroxidase	Arachidonic acid metabolism, Glutathione metabolism

(a)

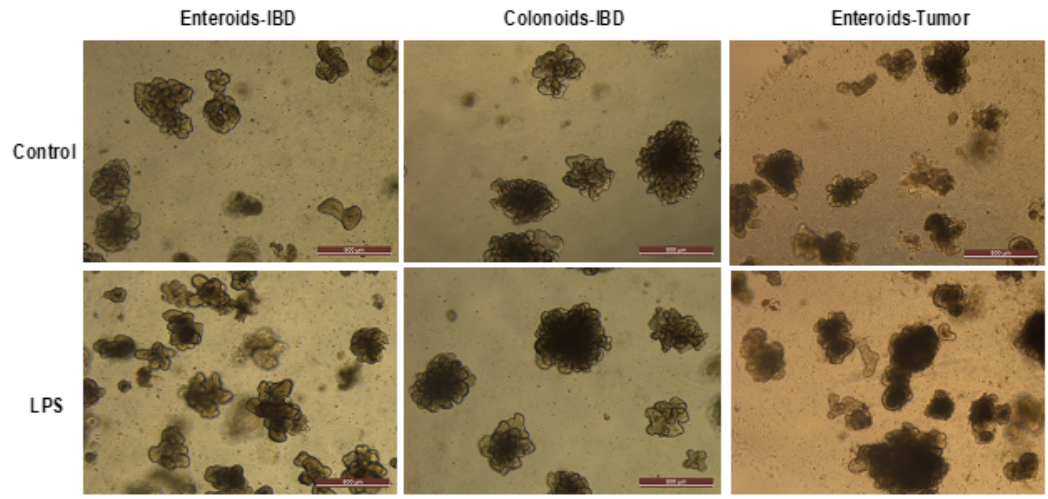

(b)

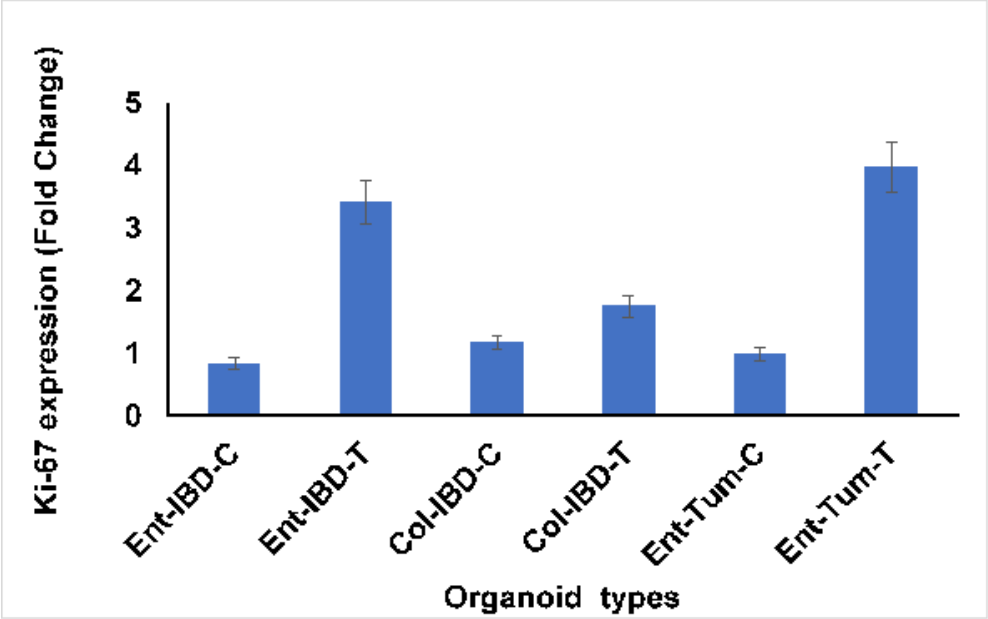

Figure 1

LPS stimulates higher proliferation.

(a) Enteroids and colonoids from dogs with IBD and intestinal mast cell tumor, 48 hours after LPS stimulation.

Representative phase-contrast images of enteroids and colonoids after LPS stimulation. The Control group received complete growth medium whereas the LPS group received LPS 5 µg/ml in complete growth medium.

(b) Expression of Ki-67 in enteroids and colonoids from dogs with IBD and intestinal mast cell tumor, 48 hours after LPS stimulation as measured by qPCR. The Control group received complete growth medium, whereas the LPS group received LPS 5 µg/ml in complete growth medium. GAPDH was used to normalize. Ent-IBD-C: control

IBD enteroids; Ent-IBD-T: IBD enteroids following LPS stimulation; Col-IBD-C: control IBD colonoids; Col-IBD-T: IBD colonoids following LPS stimulation; Ent-Tum-C: control tumor enteroids; Ent-Tum-T: tumor enteroids following LPS stimulation.

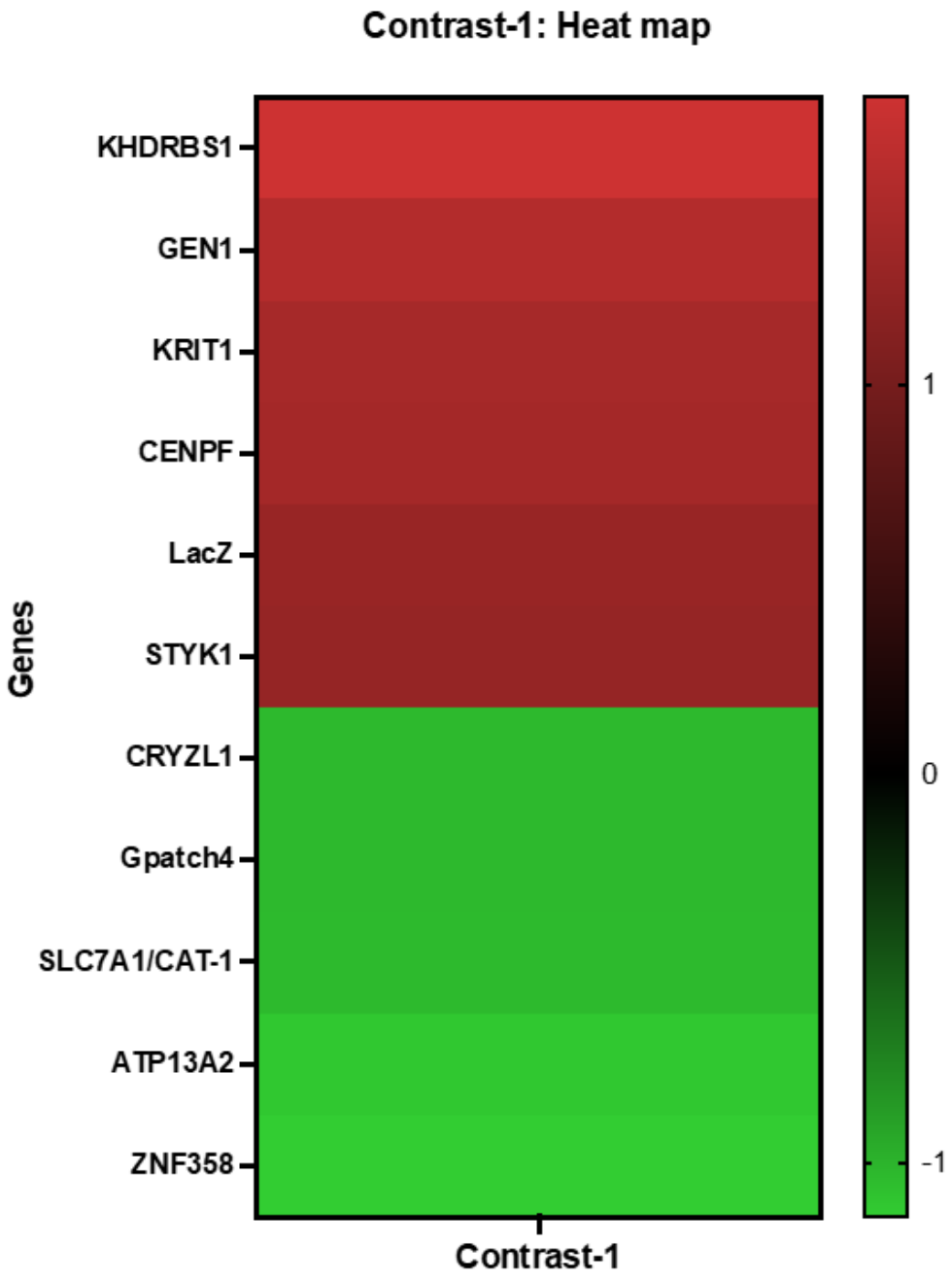

Figure 2

Heat map representing color-coded expression levels (log-ratio M values) of the top six upregulated and five downregulated DEGs in LPS treated tumor enteroids vs. control tumor enteroids (Contrast-1). The log-ratio M values represent log(R/G) (log fold change) (Tarca et al. 2006).

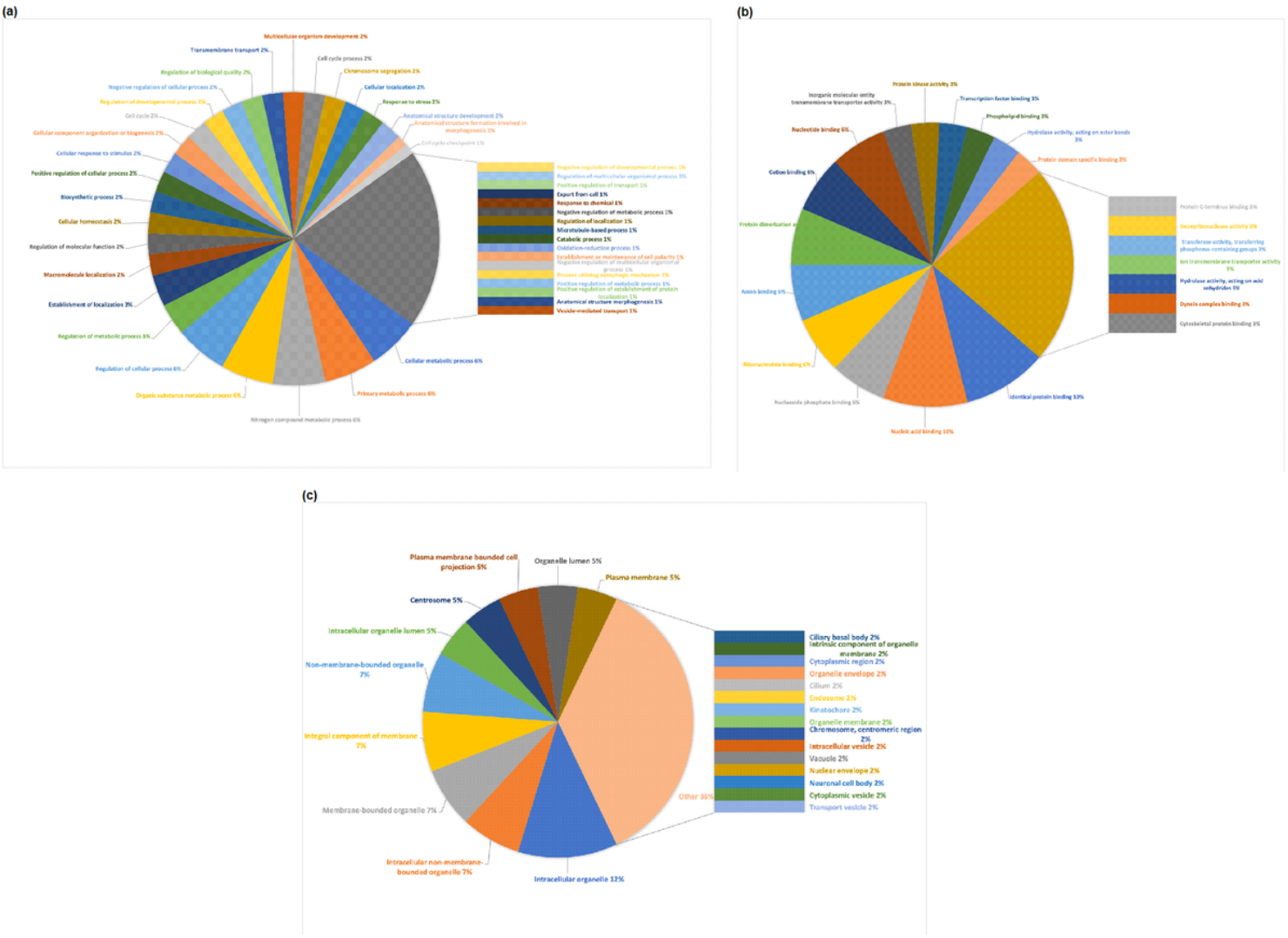

Figure 3

Gene Ontology (GO) analysis of top 10 upregulated and 10 downregulated DEGs in LPS treated tumor enteroids versus control tumor enteroids. The pie graphs show 11 genes annotated for (a) biological process, (b) molecular function, and (c) cellular component categories. The numbers in parentheses indicate the percentage of total genes in each functional category. The summary of genes in each functional category is represented in Table-S1A-C, and the detailed information of genes is presented in Table-S1D.

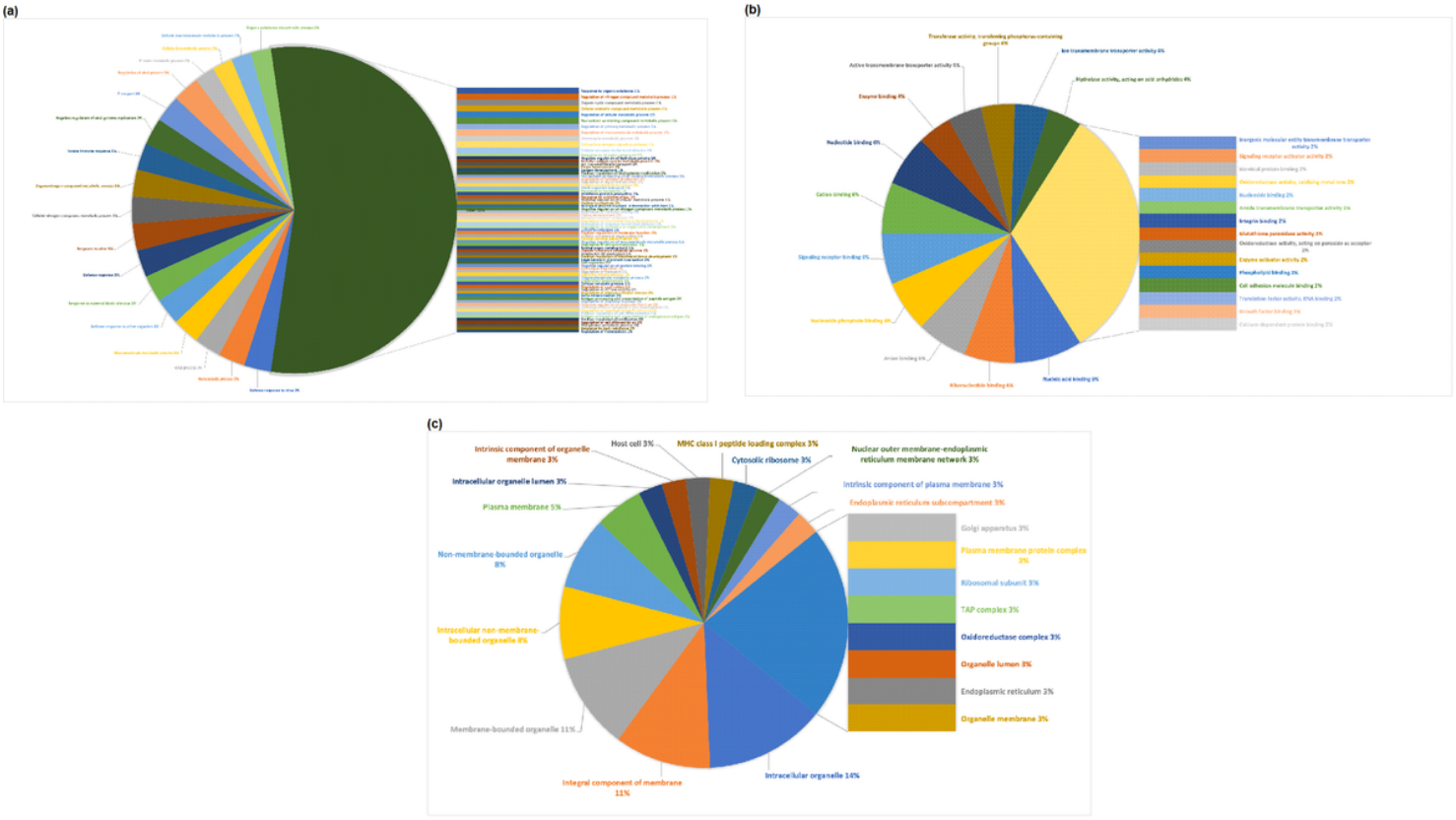

Figure 4

Gene Ontology (GO) analysis of 27 DEGs in common/same direction between IBD enteroids and colonoids following LPS stimulation. The pie graphs show DEGs annotated for (a) biological process, (b) molecular function, and (c) cellular component categories. The numbers in parentheses indicate the percentage of total genes in each functional category. The summary of genes in each functional category is represented in Table-S8A-C, and the detailed information of genes is presented in Table-S8D.

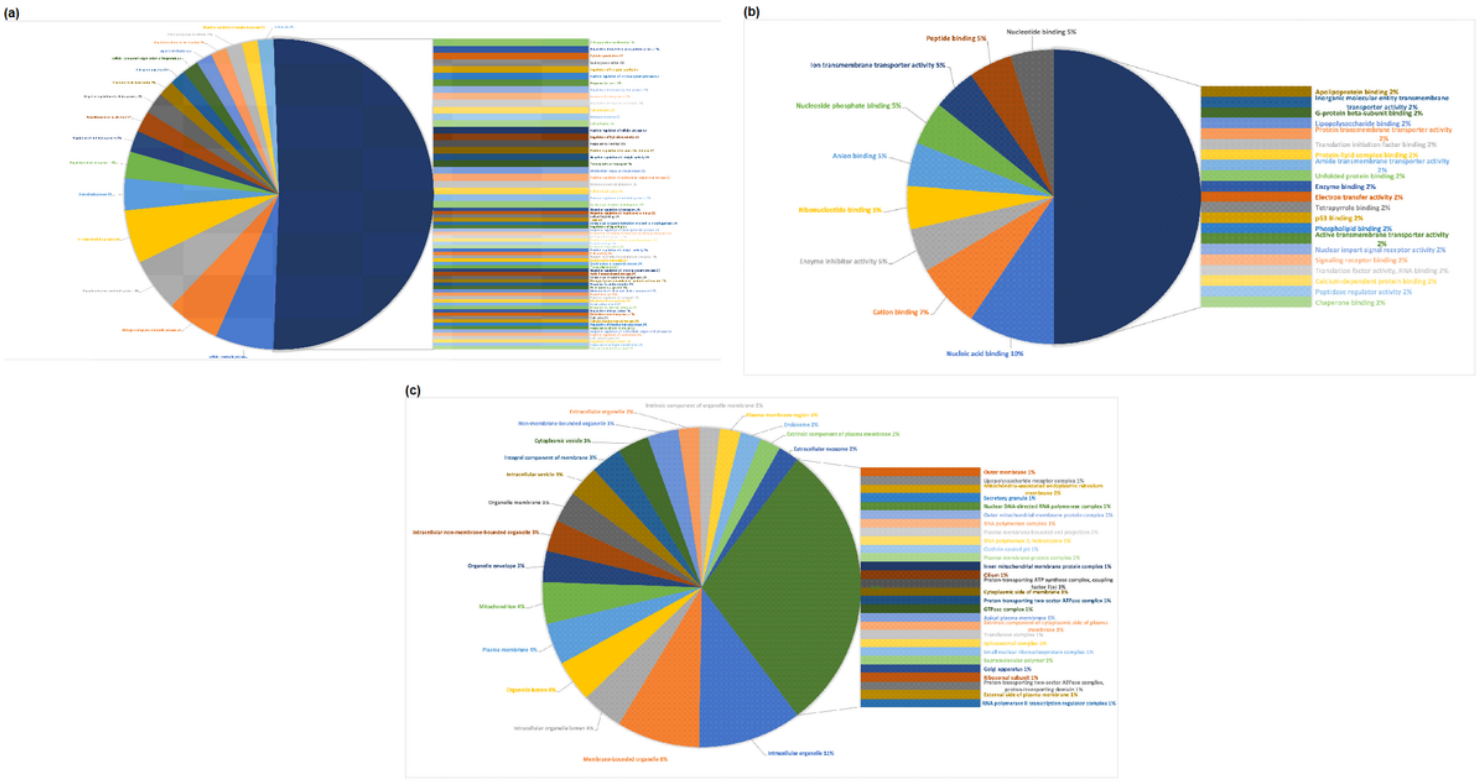

Figure 5

Gene Ontology (GO) analysis of 22 DEGs in opposite direction (upregulated in IBD enteriods and down regulated in IBD colonoids and vice versa) between IBD enteroids and colonoids following LPS stimulation. The pie graphs show DEGs annotated for (a) biological process, (b) molecular function, and (c) cellular component categories. The numbers in parentheses indicate the percentage of total genes in each functional category. The summary of genes in each functional category is represented in Table-S9A-C, and the detailed information of genes is presented in Table-S9D.

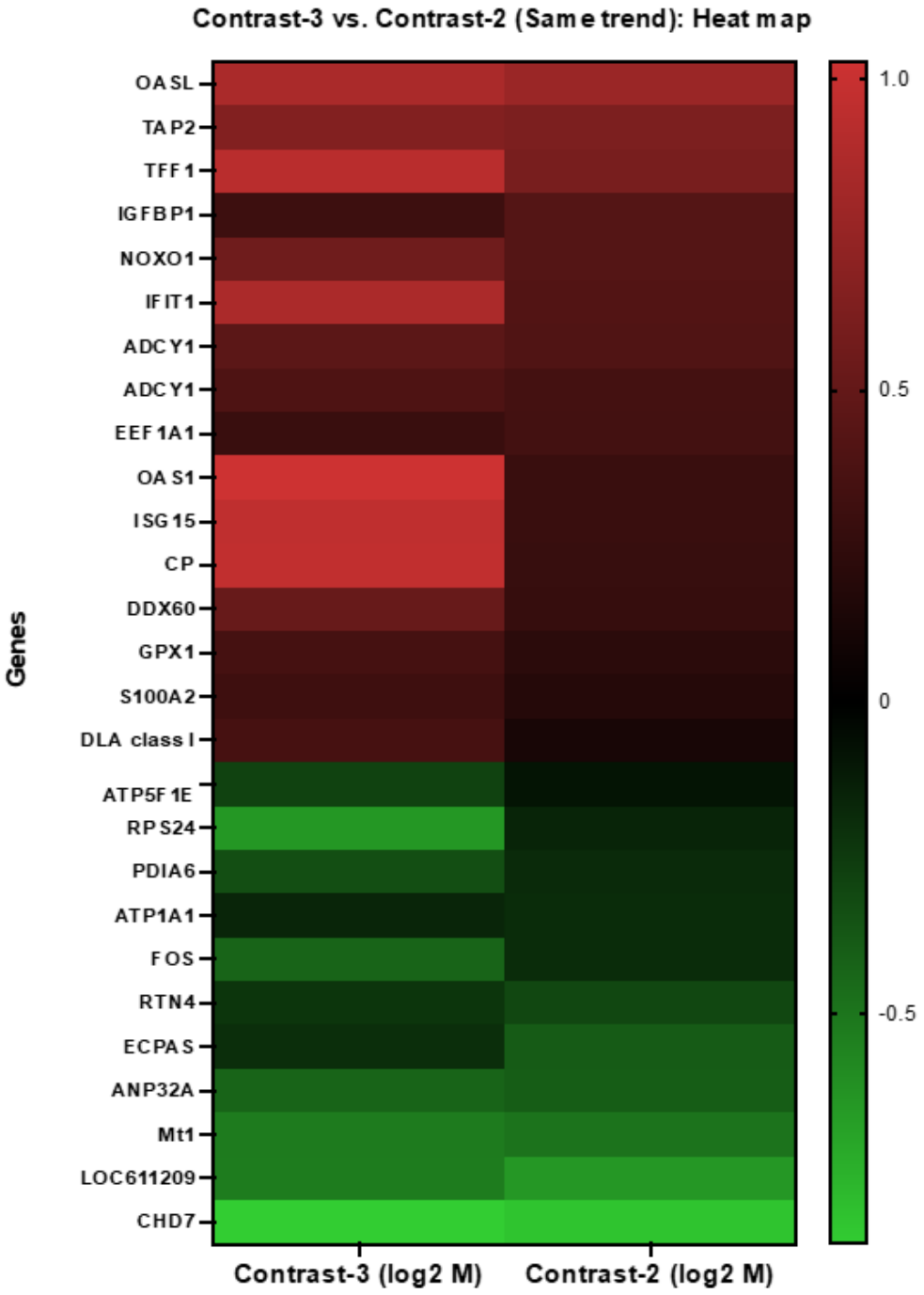

Figure 6

Heat map representing color-coded expression levels (log-ratio M values) of DEGs exhibiting similar pattern of expression between IBD enteroids and colonoids following LPS stimulation. The log-ratio *M* values represent log(R/G) (log fold change) (Tarca et al. 2006).

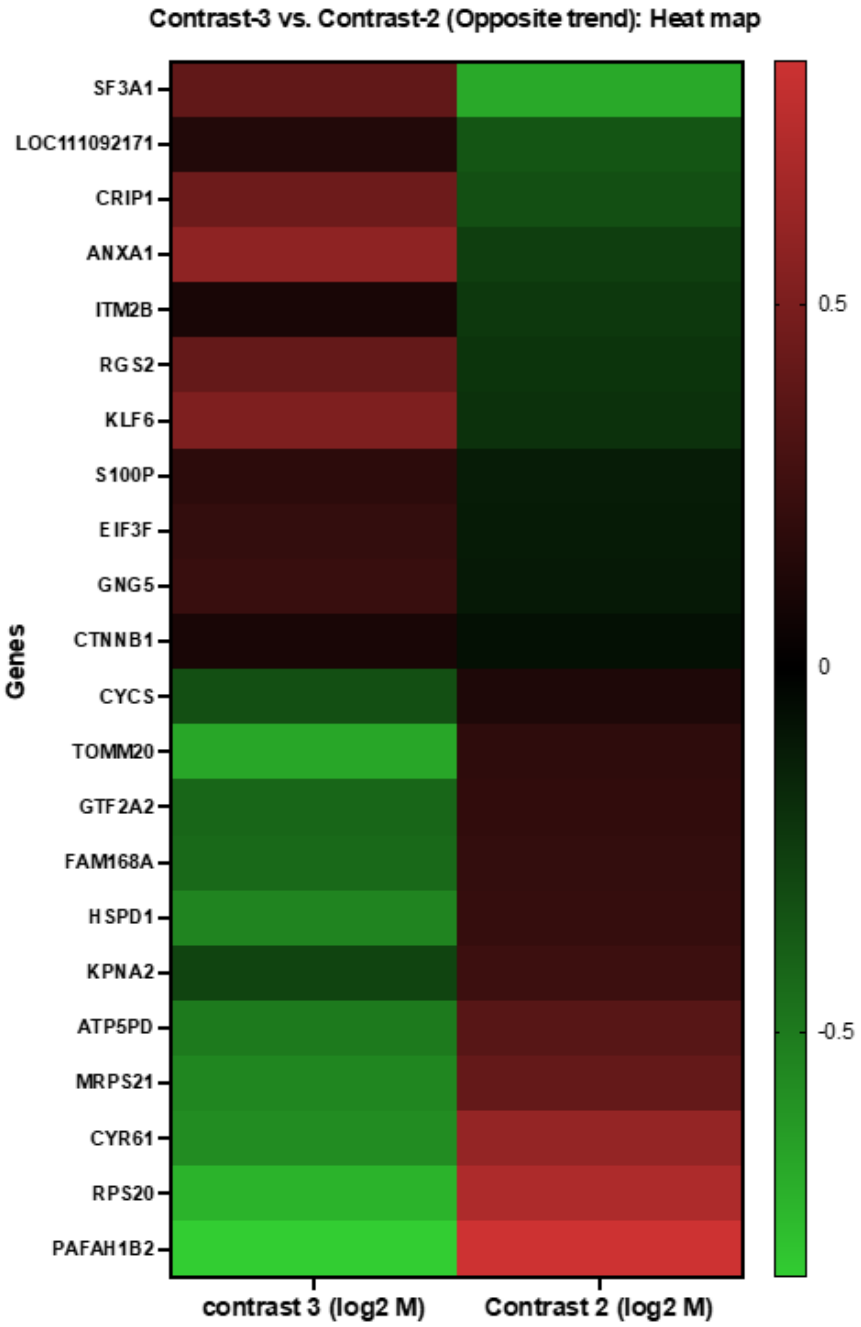

Figure 7

Heat map representing color-coded expression levels (log-ratio M values) of DEGs upregulated in IBD enteroids and down regulated in IBD colonoids and vice versa between IBD enteroids and colonoids following LPS stimulation. The log-ratio *M* values represent log(R/G) (log fold change) (Tarca et al. 2006).

Supplementary Files

This is a list of supplementary files associated with this preprint. Click to download.

- TableS1.xlsx
- TableS2.xlsx
- TableS3.xlsx
- TableS4.xlsx
- TableS5.xlsx
- TableS6.xlsx
- TableS7.xlsx
- TableS8.xlsx
- TableS9.xlsx
- FigureS1a.pdf
- FigureS10.docx
- FigureS1b.pdf
- FigureS1c.pdf
- FigureS2.docx
- FigureS3.docx
- FigureS4.docx
- FigureS5.docx
- FigureS6.docx
- FigureS7.docx
- FigureS8.docx
- FigureS9.docx
- FigureS10.docx
- SupplementalfigureLegends.docx